Response letter and revised manuscript for

"*The evolution of mode-2 internal solitary waves modulated by background shear currents*"

Peiwen Zhang, Zhenhua Xu, Qun Li, Baoshu Yin, Yijun Hou, Antony K. Liu

April 29, 2018

Dear Prof. Stastna,

On behalf of my co-authors, we greatly appreciate you and the reviewers for the constructive comments and suggestions as well as your time and efforts on processing and reviewing our manuscript. We have carefully read and consider the comments and make substantial revisions accordingly. A point by point response and the revised manuscript are provided below. In the manuscript, the main revisions were highlighted for reviewing, and a clean version of revised manuscript was uploaded separately as a supplement. We hope you find these revisions acceptable.

Some major revisions were made to address the reviewers' concern.

(1) Considering the reviewers' suggestions and comments, several important factors were investigated to generalize our research, including the magnitude, thickness of shear layer, direction, polarity and upward offset of background shear current.

(2) Abstract, results, discussion and summary were reorganized, with latest simulation results added.

(3) We added the definitions of various quantities and improved some descriptions to clarify related claims.

(4) Wrong references, typos, repetition and grammar errors were corrected. Furthermore, we also used the English editing service (NPG) to improve the language. We hope the revised manuscript advanced in readability and understanding.

Additionally, we have remapped some of the figures and improved their resolutions to make them good-quality for reading and publication, and we also have made some minor modifications on the basis of interactive discussions. We hope that you will find the revised manuscript much improved.

Thank you for your attention and consideration of our manuscript.

Yours sincerely

Dr. Zhenhua Xu

Corresponding author: Z. Xu; E-mail: xuzhenhua@qdio.ac.cn

Response to Reviewer 1:

General comments

The article presents novel numerical results describing the adjustment of a mode-2 ISW due to a background shear flow. The authors vary the center of the background shear and measure the amount of energy lost from the ISW. The authors attempt to demonstrate that this energy is radiated into three different types of waves: a leading mode-1 wave, an oscillating tail, and an amplitude-modulated wave packet. Comparison to the work of Shroyer et al. (2010) is made throughout.

The paper is well structured and contains new results that are applicable to a wide audience. However, substantial work is required to bring the paper up to an international standard. For example, there is missing literature review on mode-1 ISWs in back- ground currents and wave-mean flow interaction, various quantities are not carefully defined, and five cases do not suggest a fully developed study. Detailed suggestions and questions are below. I would like to see the article published, but the authors must address the following concerns.

Response:

Thank you very much for your constructive and helpful comments, which were extremely helpful in improving the manuscript. We have carefully read the comments and made substantial revisions accordingly as detailed in the following responses to specific questions. The NPG Language Editing service was contracted to review and polish the revised manuscript before submission. The main revisions are highlighted in the manuscript.

Question 1

There are no references to similar studies of mode-1 ISWs in shear flow. Comparisons to lower mode internal waves should be made to better position this article within the literature. Suggestions include: Stastna and Lamb (2002), and Lamb (2010).

Response:

In response to the reviewer's helpful comments, references related to mode-1 ISWs in shear flow have been added and discussed in the revision. Particularly, we have used the same method as that in *Lamb* (2010) to calculate the ISW energy in the presence of the background current. Some analysis methods in *Stastna and Lamb* (2002) are also used in the present study to investigate the variation of mode-2 wave properties in background shear current.

The related descriptions were added to the revision as follows (see also Page 2, Line 27 – Page 3, Line 5 in the main text):

"*The evolution of mode-1 ISWs in background shear current was extensively studied (Stastna and Lamb, 2002, Lamb, 2010, Grimshaw* et al.*, 2007, Fructus* et al.*, 2009). Lamb (2010) investigated the energetics of mode-1 ISWs in a background shear current, providing some methods commonly used to calculate the energy under that circumstance. Stastna and Lamb (2002) considered the effects of background current on mode-1 ISWs and discussed the properties of ISWs during the breaking process. In comparison, few works on mode-2 ISW in shear flow have been produced.*"

Question 2

Other than Shroyer et al. (2010), what other references exist for mode-2 ISWs in background currents? Are there none? That seems surprising.

Response:

Accordingly, the studies of mode-2 ISWs in the background current have been reviewed and summarized. Because of the difficulty to capture both the mode-2 waves and low-frequency background flows, to our knowledge, *Shroyer* et al. (2010)'s study is the sole one with the observational evidence based on which we can numerically examine the integrated evolution process of mode-2 ISWs in the background shear current.

The related descriptions were added to the revision as follows (see also Page 3, Lines

5 – 8; Page 3, Lines 10 – 13 in the main text):

"*Vlasenko* et al. *(2010) observed mode-2 ISW followed by short wavelength mode-1 oscillating tail in the Luzon Strait. Liu* et al. *(2013) investigated the generation and evolution of mode-2 ISW in the South China Sea and concluded that the more dispersive mode-2 ISW might not propagate, evolve and persist for long time on the shelf.*"

"*Shroyer* et al. *(2010) was the sole one recording an integrated evolution process of mode-2 ISW and found that the leading mode-2 wave quickly deformed and developed a tail of short, small-amplitude mode-1 wave in the presence of background shear current.*"

Question 3

What predictions does theory make? Do the author's results match those of weakly nonlinear theory? It appears that KdV theory will apply and much can be learned by using standard techniques of KdV theory.

Response:

The initial properties of mode-2 ISW without the presence of a background shear current in our study is consistent with the prediction by KdV (Korteweg-de Vries) theory (Figure 1) (*Grimshaw* et al., 2007). As introduced by *Maderich* et al (2010), the weakly nonlinear KdV theory is suitable for slowly varying background conditions, but the intensive evolution process is not expected in the KdV framework, and as a result, a numerical modal approach is needed (*Grimshaw* et al., 2010; *Terletkska* et al., 2016; *Yuan* et al., 2018). The recent work by *Yuan* et al., (2018) observed the existence of a long mode-1 wave ahead of the mode-2 ISW during the evolution of mode-2 ISW over variable topography and found that this process cannot be characterized by KdV theory. Therefore, in the present study, we use the full-nonlinear and nonhydrostatic MITgcm model to examine the integrated evolution process of mode-2 ISW in the background shear current.

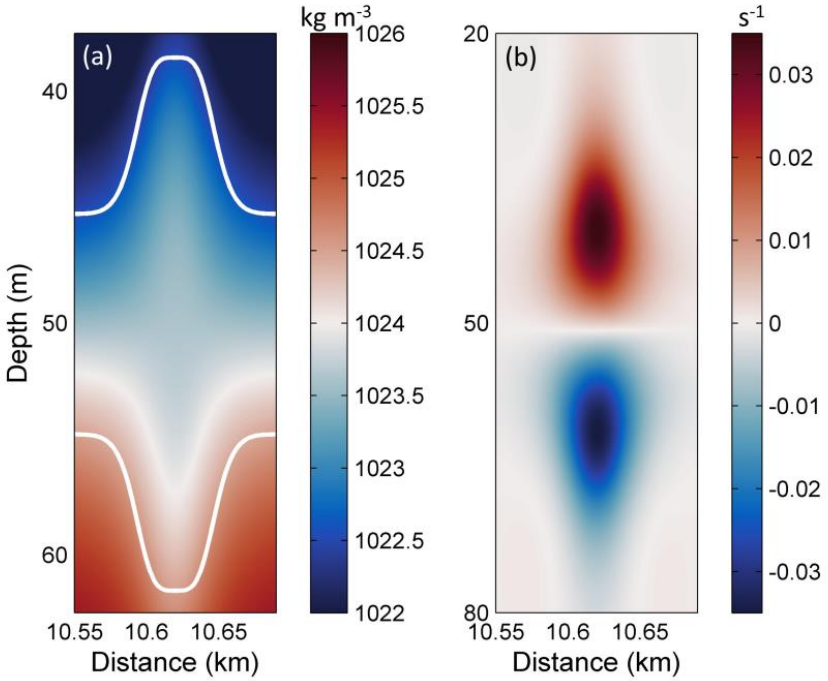

Figure 1. The characteristics of a single mode-2 ISW's (a) density field and (b) vorticity in the absence of background shear current. The white lines in (a) demonstrate the theoretical solution of mode-2 ISW in KdV framework.

The related descriptions were added to the revision as follows (see also Page 2, Lines 19 – 23 in the main text):

"*Yuan* et al. *(2018) observed the existence of a long mode-1 wave ahead of mode-2 ISW during the evolution of mode-2 ISW over variable topography and found that this process cannot be characterized by KdV theory. The authors suggested using the MITgcm model, which can solve all modes to investigate the integrated evolution process of mode-2 ISWs in variable background conditions.*"

Question 4

Do five cases provide sufficient information to make generalized claims about ISWs in shear flow? For comparison, Maderich et al. (2017) ran 35 cases of collisions of internal waves.

Response:

Thank you for the constructive suggestion. Accordingly, several important factors were investigated to generalize our research in the literature, including the magnitude, thickness of shear layer, direction and symmetric offset of background shear current. The detailed configuration of the numerical simulation is given in Table 1.

Table 1. Summary of parameters of variable background shear currents. The depth and thickness of the pycnocline are denoted by z_0 and h. The thickness of the shear layer is denoted by h_s, and the offset cases are indicated by asymmetry parameter Δ. The magnitude of the shear current is denoted by U_d. *Por* indicates the polarity of the background shear current, and "+" means a polarity-reversal shear current. The orientation of the background shear current is indicated by *Ori*, and "+" means an opposing shear current.

Case	z_0	h	h_s	Δ	U_d	*Por*	*Ori*
O1	50	10	3	-2	0.22	(-)	(-)
O2	50	10	3	-1.5	0.22	(-)	(-)
O3	50	10	3	-1	0.22	(-)	(-)
O4	50	10	3	-0.5	0.22	(-)	(-)
O5	50	10	3	0	0.22	(-)	(-)
O6	50	10	3	0.5	0.22	(-)	(-)
O7	50	10	3	1	0.22	(-)	(-)
O8	50	10	3	1.5	0.22	(-)	(-)
O9	50	10	3	2	0.22	(-)	(-)
H1	50	10	1.5	0	0.22	(-)	(-)
H2 (O5)	50	10	3	0	0.22	(-)	(-)
H3	50	10	4.5	0	0.22	(-)	(-)
H4	50	10	6	0	0.22	(-)	(-)
H5	50	10	7.5	0	0.22	(-)	(-)
U1	50	10	3	0	0.11	(-)	(-)
U2 (O5)	50	10	3	0	0.22	(-)	(-)
U3	50	10	3	0	0.33	(-)	(-)
U4	50	10	3	0	0.44	(-)	(-)

U5	50	10	3	0	0.55	(-)	(-)
D1	50	10	3	0	0.22	(-)	(+)
P1	50	10	3	0	0.22	(+)	(-)

The related descriptions were added to the revision as follows (see also Page 3, Lines 17 – 21; Page 5, Lines 2 – 7 in the main text):

"*To reveal the sensitivity of the evolution of mode-2 ISWs to variable parameters of background shear currents, we introduced five sets of experiments (21 experiments in total) to generalize our research, including the magnitude, thickness of the shear layer, direction and offset (centre of the shear layer relative to the centre of the pycnocline) of the background shear current."*

"In the sensitive experiments, the magnitude of the shear current is denoted by U_d *and defined as* $|\Delta U|$*. This value was varied from 0.5*U_d *to 2.5* U_d *in the sensitivity test. Similarly, the thickness of the shear layer was varied from 0.5* h_s *to 2.5* h_s*. In cases D1 and P1, an opposing and polarity-reversal background shear currents were initialized for examination, respectively. We further introduced an asymmetry parameter* Δ *to investigate the evolution of mode-2 ISWs in the offset background shear current (Carpenter* et al.*, 2010).*"

Question 5

How were the values of the shear chosen? Were they chosen to match flow on the New Jersey shelf? What would happen if the shear was varied in terms of magnitude, or was oriented against the ISW (such that U1 and/or U2 were positive). What about shifting the shear upwards rather than down? What about hs compared to h? Please add some of these cases into the article. Further motivation for the values is required.

Response:

In the case O5, which was taken as a control experiment, the values of background

shear current were chosen to match the observations in the New Jersey Shelf (*Shroyer* et al., 2010). The evolution process and calculated energy loss rate for the control experiment were in relative agreement with the field observations.

According to the reviewer's suggestions in questions 4 and 5, we have run more sensitive experiments in the revision (14 additional experiments in total). The main results include the following:

Orientation

The background shear current oriented against the mode-2 ISW only slightly affects the amplitude of the forward-propagating long wave and oscillating tail but significantly influences the amplitude of the amplitude-modulated wave packet. The opposing background shear current slightly increased the energy loss of mode-2 ISW during the modulation.

Magnitude of the shear

The amplitudes of the forward-propagating long wave and amplitude-modulated wave packet are positively proportional to the magnitude of the background shear current, but the oscillating tail is not very sensitive to the increasing magnitude of the background shear current (Figure 2 (a)). The energy losses of mode-2 ISW are also positively proportional to the magnitude of the background shear current (Figure 3 (a)).

Thickness of the shear layer

The amplitudes of all three shear-induced wave structures are negatively proportional to the thickness of the shear layer (Figure 2 (b)). The energy losses of mode-2 ISW are also negatively proportional to the thickness of the shear layer (Figure 3 (b)).

Offset upward

When the shear current is offset upward, the variation of the oscillating tail and amplitude-modulated wave packet in amplitude show similar trends to the downward offset cases (Figure 2 (c) and (d)), but the forward-propagating long wave is still insensitive to the offset direction of the shear current (Figure 2 (c) and (d)). The energy losses of mode-2 ISW are also negatively proportional to the asymmetry parameter Δ in both upward and downward conditions (Figure 3(c) and (d)).

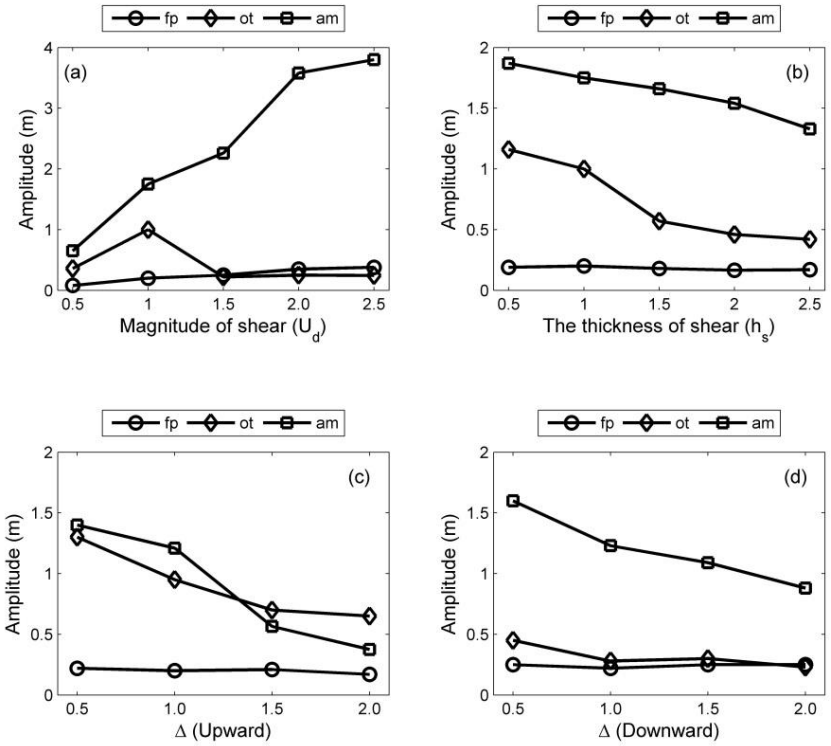

Figure 2. The summarized results of the amplitudes of the forward-propagating long wave (denoted by 'fp'), oscillating tail (denoted by 'ot') and amplitude-modulated wave packet (denoted by 'am') with the presence of (a) varied magnitude of shear currents at 40 T, (b) varied thickness of shear currents at 40 T, (c) upward offset background shear currents at 30 T and (d) downward offset background shear currents at 30 T.

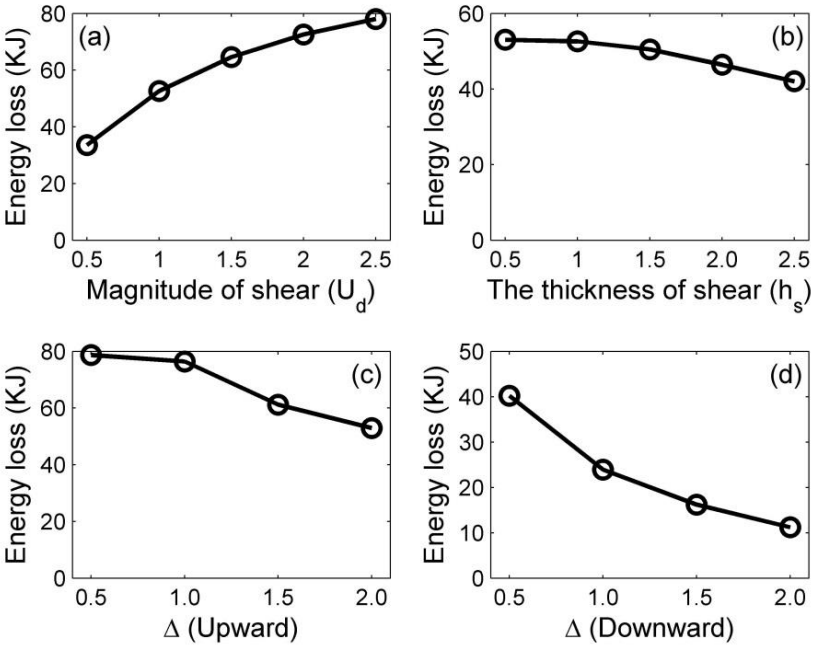

Figure 3. The summarized results of the energy loss of the mode-2 ISW at 30 T with the presence of (a) varied magnitude of shear currents, (b) varied thickness of shear currents, (c) upward offset background shear currents and (d) downward offset background shear currents.

The related descriptions were added to the revision as follows (see also Page 4，Lines 14 – 15; Page 13, Lines 14 – 21; Page 14, Lines 1 - 14; Page 14, Line 20 – Page 15, Line 6; Page 13 Lines 3 - 9; Page 15, Lines 8 – 17; Page 15, Line 27 – Page 16, Line 3; Page 22, Lines 2 – 13 in the main text):

"*The choice of background density stratification in all experiments and the shear current in the control experiment (case O5) followed the field observation over the New Jersey Shelf (Shroyer* et al.*, 2010).*"

"*In case D1, the background shear current oriented against the mode-2 ISW. The general pattern of the forward-propagating long wave, oscillating tail and amplitude-modulated wave packet were similar to those in the control experiment. In this opposing case D1, the amplitude of the forward-propagating long wave and oscillating tail were not significantly affected. For the mode-2 ISW, its amplitude also remains nearly unchanged between the following and opposing cases, while the amplitude-modulated wave packet's amplitude decreased from 1.85 m (following case) to 1.09 m in the opposing case. These results suggest that only the amplitude-modulated wave packet is sensitive to the orientation of the background shear current.* "

"*The magnitude of the background shear current was varied from 0.5* U_d *to 2.5* U_d *from case U1 to case U5 to study its influence on the evolution of the mode-2 ISW. In case U5 (Fig. 9), a relatively larger amplitude forward-propagating long wave was observed at 20 T (Fig. 9 (c)). The mode-2 ISW became inconspicuous at 50 T (Fig. 9 (d)), while an amplitude-modulated wave packet propagated clearly. The increasing magnitude of the background shear current leads to smaller amplitudes of the mode-2 ISW in both upper and lower parts. In the larger magnitude case, the*

amplitude-modulated wave packet and forward-propagating long wave were significantly strengthened, and their amplitudes reached 3.75 m and 0.38 m (case U5), respectively. In contrast, a larger magnitude didn't make the amplitude of the oscillating tail continue to increase. In the larger magnitude case, the oscillating tail was unable to be clearly observed. Its amplitude becomes smaller (0.25 m) than that of the forward-propagating long wave (0.38 m). In summary, all three shear-induced waves are sensitive to the magnitude of the shear current."

"*The thickness of the shear layer h_s was also varied to investigate its effect on the modulation of mode-2 ISW (cases H1 to H5). In comparison with the control experiment, the forward-propagating long wave's amplitude decreased with larger h_s, reaching 0.17 m in case H5 with 2.5 h_s. The amplitude-modulated wave packet and oscillating tail both decrease to 1.33 m and 0.42 m in amplitude in larger h_s (case H5), respectively, while the mode-2 ISW's amplitude reaches 7.95 m. This result shows that the background shear current with smaller h_s could only moderately deform the mode-2 ISW. As a result, all three shear-induced wave structures are sensitive to the variation in the thickness of the shear layer.*"

"*When the shear current is offset in the upward direction ($\Delta < 0$), the asymmetry of the mode-2 ISW during the modulation became clearer. The amplitude of the oscillating tail and amplitude-modulated wave packet both decreased when the shear current was offset upward, showing a symmetric variation trend with respect to the downward offset condition. For the forward-propagating long wave, its amplitude oscillates by approximately 0.2 m, suggesting the insensitive nature of the long wave to the upward offset shear current.*"

"*The amplitudes of the forward-propagating long wave, oscillating tail and amplitude-modulated wave packet in varied background shear currents are summarized to investigate their sensitivity to the varied background shear currents. The amplitude of the forward-propagating long wave and amplitude-modulated wave*

packet are positively proportional to the magnitude of the background shear current, but the oscillating tail is insensitive to the higher magnitude of background shear current (Fig. 10 (a)). The amplitudes of the oscillating tails and amplitude-modulated wave packet are inversely proportional to the thickness of the shear layer, and the forward-propagating long wave decreased slightly in amplitude with increasing h_s *(Fig. 10 (b)). To reveal the effects of the* Δ *on those shear-induced wave structures, a comparison of different cases from* $\Delta = 0$ *(case O5) to* $\Delta = 2$ *(case O9) was given.*"

"*A similar variation trend could be found in the upward offset cases (Fig. 10 (c)). The amplitudes of the oscillating tail and amplitude-modulated wave packet decreased monotonically as the shear current offset upward. The forward-propagating long wave was barely affected by* Δ *and remained constant at approximately 0.2 m in all offset cases.*"

"*The polarity and the direction of the background shear current have minor effect on the energy loss of mode-2 ISWs. The energy loss of the mode-2 ISW was positively proportional to the magnitude of shear current, but reverse proportional to the thickness of shear layer (Fig. 15 (a) and (b)). For case U5, 78.04 KJ* m^{-1} *energy loss in 30 T, ~53% of total energy of mode-2 ISW and the averaged energy loss rate was 13* Wm^{-1}*, indicating the magnitude of shear could significantly increase the energy loss of mode-2 ISW. in contrast, for case H5, 42.05 KJ* m^{-1} *energy loss in 30 T, ~29% of total energy of mode-2 ISW and the averaged energy loss rate was 7W* m^{-1}*, showing that a larger thickness of shear has opposite effect on the energy loss of mode-2 ISW. In the offset background shear currents, the energy loss of mode-2 ISW monotonically decreased with an increasing* Δ*, showing a symmetric trend in both upward and downward offset cases (Fig. 15 (c) and (d)). Therefore, the energy losses of mode-2 ISWs are sensitive to the magnitude, thickness and offset extent, but insensitive to the polarity and direction of background shear current."*

Question 6

How was the background shear introduced? Was it continuously increased over a short duration of time or instantaneously turned on? What was numerically done to add the shear? The first paragraph of section 2.3 does not make it clear that the ISW was generated without the presence of the background shear. Please correct this.

Response:

The initialization of the mode-2 ISW in section 2.3 has been refined accordingly. The background shear current was instantaneously turned on after the appearance of a stable mode-2 ISW in the absence of a background shear current. Then, the velocity field of the background shear current was superimposed on the model.

The related descriptions were added to the revision as follows (see also Page 6, Lines 1 – 2, Page 7 Lines 9 – 11 in the main text):

"*A rank-ordered mode-2 ISW train was generated by the "lock-release" method without background current.*"

"*At 6000 s after the initialization of numerical model, the velocity field of the background shear current was superimposed on the model.*"

Question 7

Page 7, line 4. How was the amplitude of the wave calculated? Much of section 3 discusses the change in amplitude or compares different amplitudes, but it is unclear where this came from. L is also not defined in the text.

Response:

The definitions and calculations of the amplitude have been clarified accordingly, and the definition of *L* has been added in the manuscript.

The related descriptions were added to the revision as follows (see also Page 10, Lines 6 – 8; Page 7, Lines 6 - 9 in the main text):

"*The amplitudes of shear-induced waves were defined as maximum isopycnal displacement (Stastna and Lamb, 2002).*"

"The amplitude A of mode-2 ISWs was defined as the maximum displacement of the upper and lower isopycnals, which are equal in the initial state (Terletska et al.*, 2016). The wavelength L was defined as the width of the wave at half of the amplitude of the mode-2 ISW in the initial state.*"

Question 8

What is the difference between the oscillating tail and the amplitude-modulated wave packet? To me they look identical. What are their defining features? How did you distinguish between them?

Response:

Detailed definitions of the oscillating tail and amplitude-modulated wave packet have been added in the revision. The related figures have been improved to clearly demonstrate their differences. The amplitude-modulated wave packet appeared at the end of oscillating tail as steady-state envelopes *(Terletska* et al., 2016), and it could be clearly observed at the end of the oscillating tail (Figure 4). The amplitude-modulated wave packet (Figure 5) was defined as a pulsating wave packet propagated with a steady-state envelope, inside which the waves oscillate freely with different amplitudes (*Terletska* et al., 2016).

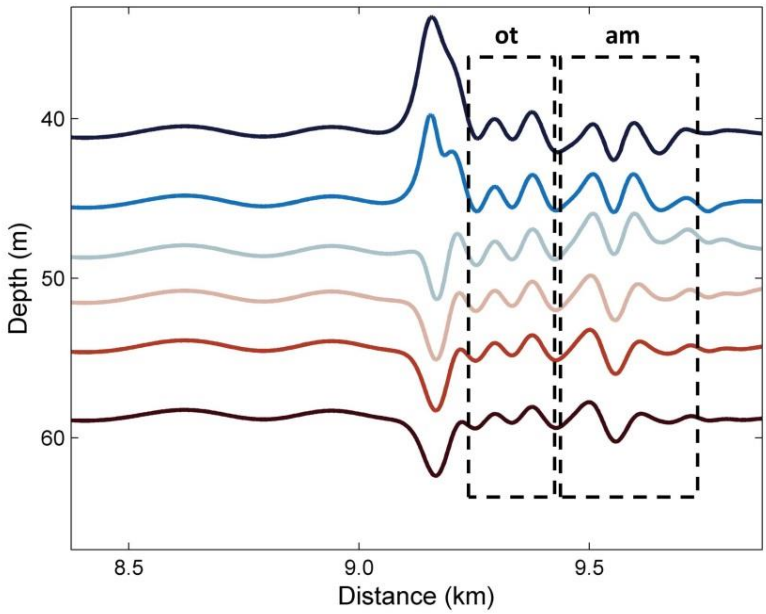

Figure 4: The evolution process of mode-2 ISW in case O5 at 14 T, where the 'ot' and 'am' denoted the oscillating tail and amplitude-modulated wave packet, respectively (see also FIigure 4(d) in the manuscript).

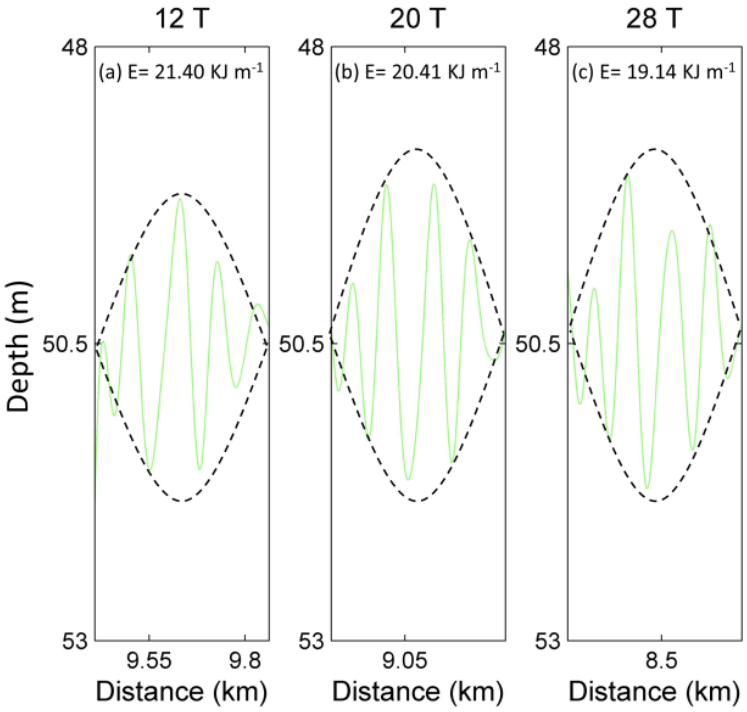

Figure 5. The envelopes of the amplitude-modulated wave packet in the case O5 (Δ = 0) at (a) 12 T, (b) 20 T and (c) 28 T, where the mean density isopycnal of upper and lower layer (green line) are plotted.

The related descriptions were added to the revision as follows (see also Page 9, Line 10 – Page 10 Line 2; Page 10, Lines 11 – 13 in the main text):

"*It also caused the asymmetrical distribution of the vorticity in the horizontal, which*

is associated with the generation of forward-propagating long waves and the amplitude-modulated wave packet (Fig. 4 (b)), and the latter was defined as a pulsating wave packet (Clarke et al.*, 2000). The pulsating wave packet propagated with a steady-state envelope, inside which the waves oscillate freely with different amplitudes (Terletska* et al.*, 2016).*"

"*The oscillating tail caused by the shear was visible between the mode-2 ISW and the amplitude-modulated wave packet (Fig. 5 (d)) at 14 T, and it was a radiated mode-1 oscillatory disturbance trailing mode-2 ISW (Stamp and Jacka, 1995).*"

Question 9

Page 9, lines 9-16. How does the complexity of the vorticity field imply higher energy transfer? How do you know that the energy in the radiating waves does not arise from the background mean flow? Have the authors read the literature on wave-mean flow interaction? This seems highly pertinent and must be included in the article. Lastly, how does larger amplitude imply a higher energy? Are the authors assuming linearity? Is this applicable here? The use of the term applied (or implying) in these sentences is not justified, and begs further quantification. (See also lines 18-21 on page 11).

Response:

Thank you for your suggestion. The vague description of the relationship between the complexity of vorticity and the energy transfer has been revised. The linear relation between energy and amplitude is inappropriate here, and it has been improved accordingly.

We reviewed some classic works on wave-mean flow interaction. Then, we compared the energy loss of mode-2 ISWs with the total energy of radiating waves and found they were nearly the same in quantity. This finding means that the energy from the background mean flow makes a relatively small contribution to the radiating waves. To reveal the energy transfer process in wave-mean flow interactions require a detailed analysis, but this is beyond the main scope of present study, which focused on

the evolution of mode-2 ISWs in the background shear current. A comment has been added to the manuscript that notes the importance of wave-flow interaction investigations in the near future.

The related descriptions were added to the revision as follows (see also Page 10, Lines 2 – 10; Page 13, Lines 9 – 11; Page 27, Lines 22 – 24 in the main text):

"*To the aft of the ISW, the shear induced by the background currents lead to the deformation of the vortex dipole, and an increasing complexity of the vorticity field implied an intensive adjustment occurred. As illustrated in Fig. 5 (c), the vorticity of the mode-2 ISW is redistributed to adapt to the background condition at 10 T. In this process, the vortex of the ISW shrank with the generation of an amplitude-modulated wave packet and a forward-propagating long wave. The amplitudes of shear-induced waves were defined as maximum isopycnal displacement (Stastna and Lamb, 2002). The forward-propagating long wave and amplitude-modulated wave packet can be seen in Fig. 5 (c) with amplitudes of 0.25 m and 1.8 m respectively, and the latter was clearly observed at the rear of the mode-2 ISW.*"

"*The small amplitude of the oscillating tail and amplitude-modulated wave packet indicate that the modulation could be weaker when* Δ *increased, and the weakening of the oscillating tail makes the amplitude-modulated wave packet more visible.*"

"*In future work, a possible avenue is the evolution of mode-2 ISW in time-varied background shear current, and the wave-mean flow interaction in this complicated flow fields, revealing the energy exchange process between waves and mean-flow."*

Question 10

In connection to the previous comment, section 3.4 makes many of the same assumptions about how energy and wave amplitude are related. But this relation is unclear and non-trivial.

Response:

The descriptions in section 3.4 have been improved accordingly. We have also optimized the structure of the manuscript to include the relationship between the amplitudes of shear-induced waves with different parameters of background shear currents, and the energy analysis has been moved to the following sections.

The related descriptions were added to the revision as follows (see also Page 15, Lines 17 – 26 in the main text):

"*The modulation caused by background shear currents was weakened as the Δ increased, corresponding to the decreased amplitude of the amplitude-modulated wave packet and oscillating tail. The amplitude-modulated wave packet has the highest amplitude among all cases compared to those of the other two wave forms. The amplitude of the amplitude-modulated wave packet decreased from 1.8 to 1 m monotonically, and the amplitudes of the oscillating tails decreased from 0.85 to 0.25 m between the case O5 (Δ = 0) and the case O7 (Δ = 1) but remained stable between the case O7 (Δ = 1) and case O9 (Δ = 2), indicating that the amplitude-modulated wave packet were more sensitive to the Δ than the oscillating tail. As expected, the ratio between the amplitude of modulated wave packet and oscillating tails increased from 2.1 in the case O5 to 4 in the case O9, so the amplitude-modulated wave packet became more distinct in case O9."*

Question 11

Page 9, lines 20-22. The consequent in the following conditional sentence does not following from the antecedent. "Based on the vorticity field shown in Fig. 6 (d), the generation of the oscillating tail and the forward-propagating long wave was continuously sustained by the energy of the ISW". A single snapshot does not indicate anything about the continuous evolution of the radiating waves. I suggest adding a Hovmoller (space-time) plot to show the time varying nature of the waves. However, this is only possible if sufficient time resolution is available.

Response:

Thank you for your suggestion. A Hovmöller plot has been made to illustrate the time-varying nature of the evolution process of the mode-2 ISW (Figure 6). The oscillating tail and forward-propagating long wave could be found to evolve continuously. Related descriptions have been added to the manuscript.

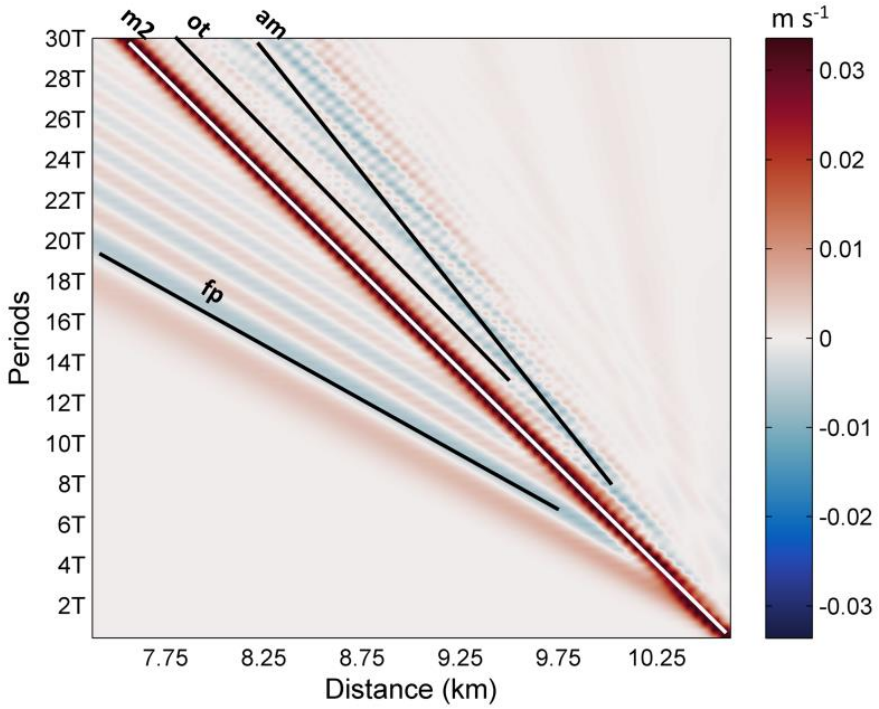

Figure 6. Hovmöller plot of horizontal velocity without background shear current at the surface. The mode-2 ISW, forward-propagating long wave, oscillating tail and amplitude-modulated wave packet are denoted by 'm2', 'fp', 'ot' and 'am', respectively.

The related descriptions were added to the revision as follows (see also Page 10, Lines 13 - 15; Page 10, Lines 16 – 20 in the main text):

"*A Hovmöller plot (Fig. 6) of horizontal velocity without the background shear current at the surface was plotted. The forward-propagating long wave, oscillating tail and amplitude-modulated wave packet were found to propagate persistently.*"

"*Based on the vorticity field (Fig. 5 (d)) and the time-space varying nature (Fig. 6), the generation of the oscillating tail and forward-propagating long wave were continuously sustained by the energy of the ISW with decreasing rate. Therefore, they*

have the potential to drain the energy from an ISW over a long time scale."

Question 12

Page 13. How are x_l and x_r defined? The authors say they are the boundaries of the integration region, but don't specify where they come from. They are critical to the discussion of the size of the wave, and the choice of definition will have a large impact in the energy values.

Response:

The definitions of x_l and x_r have been clarified. x_l and x_r are denoted the as the left and right boundaries, respectively, where the available potential energy flux equals zero (*Lamb*, 2010).

The related descriptions were added to the revision as follows (see also Page 17 Lines 7 - 9 in the main text):

"*x_r and x_l are the boundary locations of the integration region, and x satisfies $x_l \leq x \leq x_r$. During the calculation of the wave energy, x_r and x_l are denoted as the left and right boundaries, respectively, where the available potential energy flux equals zero (Lamb, 2010)*"

Question 13

Page 20, lines 9-11. What waves are transient to the introduction of the shear, and what are persistent? Much of this article seems to consist of the initial adjustment when the background shear is introduced. What is the long time behavior of the mode-2 wave in the presence of shear? On another note, what can be said about the generation of a mode-2 ISW while shear is present?

Response:

The amplitude-modulated wave packet, oscillating tail and forward-propagating long wave were observed to be persistent (Figure 6). The forward-propagating long wave

and oscillating tail are generated persistently due to the continuous energy input from mode-2 ISW (Figure 6). The amplitude-modulated wave packet is generated transiently because it no longer receives energy from the mode-2 ISW after it propagates away.

As for the long-term behaviour, the mode-2 ISW could adjust itself to adapt to new background conditions if there exists a stable solution for the mode-2 ISW. In contrast, the energy of mode-2 ISW would radiate away if no stable solution for the mode-2 ISW is allowed in that circumstance. This dynamic also indicates that the mode-2 ISW could generate in an appropriate background shear current where a stable solution exists. A detailed discussion has been added in the manuscript.

The related descriptions were added to the revision as follows (see also Page 26, Lines 9 – Page 27, Line 1 in the main text):

"*As for the long-term behaviour, the mode-2 ISW could adjust itself to adapt to new background conditions and experience a dramatic transformation with disintegration into a wave train (Grimshaw* et al.*, 2010, Yuan* et al.*, 2018). In our simulation, the mode-2 ISW was observed to adjust itself to the new background condition with a shear current. The high energy loss rate is in agreement with the observation by Shroyer* et al. *(2010). However, the mode-2 ISW might not be able to survive for long time in situ because the background conditions in real ocean could be more complex and vary with time, leading to a background condition where a stable solution of mode-2 ISW does not exist. "*

Specific comments

Question 1

Page 3, lines 12-14. Are there references?

Response:

Related references have been cited.

Question 2

Page 4, what evidence do you have that your solution is numerically convergent or accurate? Did you conduct grid refinement strategies? How were the viscosity parameters chosen? What motivation do you have for them?

Response:

The total energy of simulation domain has been integrated, and we found that it was convergent and stable. The initial mode-2 ISW in the absence of a background shear current was also in agreement with the KdV theory (Figure 1).

Second, no grid refinement strategies were applied. A high resolution was introduced to assure that the modulation of the mode-2 ISW in the background shear current could be clearly observed. The time-step of the simulation was set 0.4 s to satisfy the *Courant-Friedrichs-Lewy* condition.

The choice of viscosity was set following previous studies with similar field scales (*Grisouard et al.*, 2010, *Xie et al*., 2015). The choice of viscosity aims to avoid breaking and ensure the model can run smoothly (*Guo* and *Chen*, 2012, *Yuan* et al., 2018).

Question 3

Page 4, line 19. Please write the equation for delta out explicitly.

Response:

The equation for Δ has been added.

The related descriptions were added to the revision as follows (see also Page 5, Lines 5 – 8 in the main text):

"*The asymmetry parameter Δ is defined as follows:*

$$\Delta = \frac{D_s - z_0}{h/2}$$

where D_s *denotes the depth of shear centre and* h *denotes the thickness of*

pycnocline."

Question 4

Figure 1. Please define the cases in the main body of the article and not in the figure caption.

Response:

A detailed introduction of experiments has been added in the revision.

The related descriptions were added to the revision as follows (see also Lines Page 5, Lines 9 – 11 in the main text):

"*Δ was varie*d *from -2 to 2 (case O1 to case O9) to investigate the evolution of the mode-2 ISW in the offset background shear current.*"

Question 5

h_{mix} and l_{mix} are not defined in the text. Just in the caption for figure 3.

Response:

The definitions have been added.

The related descriptions were added to the revision as follows (see also Page 7, Lines 1 – 3 in the main text):

"*Figure 3 demonstrates a schematic diagram of initialization process and the configuration of model parameters. A mixed region was set to be symmetric around the centreline of the pycnocline at the right end, and its length* l_{mix} *and height* h_{mix} *were 375 m and 25 m, respectively.*"

Question 6

Is a lock-release of this form applicable on a field scale?

Response:

The mode-2 ISW generated by ‘lock-release’ method in our simulation remains stable and demonstrates a symmetric nature in agreement with the theory (Figure 1) and consistent with the observations (*Shoryer* et al., 2010).

Question 7

The colormap used in figures 4, 6, 8 is not good. Please change to something symmetric about a reference value. I suggest colormap ‘balance’ from Thyng et al. 2016. A matlab package is available for download.

Response:

We appreciate that constructive suggestion from the reviewer. We have applied the ‘balance’ colormap in the related figures accordingly.

Question 8

What is being plotted in figure 4a? Is it temperature? Please make clear.

Response:

Figure 4a shows the density field of mode-2 ISW. The caption has been modified.

Question 9

Text in figures 5, 6, etc. is too small and the resolution needs to be increased.

Response:

Revised accordingly.

Question 10

Put color bars on all vorticity plots.

Response:

Added.

Question 11

Page 10, lines 2-3. I do not see how the following sentence arises from the statement just prior to it, "Thus, the energy loss of the ISW caused by forward-propagating long waves occurs earlier than oscillating tail." I don't see how the forward-propagating wave happens earlier.

Response:

This sentence has been improved in the revision. As shown in the Hovmöller plot (Figure 6), the forward-propagating long wave and amplitude-modulated wave packet generated simultaneously. The oscillating tail appeared after the amplitude-modulated wave packet propagated away from the mode-2 ISW, indicating that the energy loss caused by oscillating tail happened later than forward-propagating long wave.

The related descriptions were added to the revision as follows (see also Page 10, Lines 20 – 24 in the main text):

"*It should be noted that the forward-propagating long wave and amplitude-modulated wave packet generated simultaneously, while the oscillating tail appeared after the amplitude-modulated wave packet propagated away from the mode-2 ISW. Thus, the energy loss of the ISW caused by forward-propagating long waves occurs earlier than the oscillating tail.*"

Question 12

Figure 8. What is BLIW? Define this somewhere.

Response:

The word 'BLIW' was changed to 'amplitude-modulated wave packet', which is more easily understood.

Question 13

Page 11, line 16. Do the authors have any physical reason why "the forward-propagating long wave may not be affected by delta"?

Response:

As suggested by reviewer, we carried out sufficient experiments to further investigate the forward-propagating long wave that was generated by the collapse of mixing induced by shear instability. The results show that the amplitude of the forward-propagating long wave is proportional to the magnitude of the shear current, indicating that the forward-propagating long wave was affected by the strength of shear. Δ denoted the offset extent of background shear current, and the strength of shear remains unchanged when Δ varied. Therefore, the variation in Δ has no effect on the forward-propagating long wave.

The related descriptions were added to the revision as follows (see also Page 24, Lines 17 – 21 in the main text):

"*The results in section 3.7 show that the amplitude of the forward-propagating long wave is proportional to the magnitude of the shear current, indicating that the forward-propagating long wave was affected by the strength of shear. Δ denotes the offset extent of the background shear current, and the strength of the shear remains unchanged when Δ varied. Therefore, the forward-propagating long wave was insensitive to variation in Δ.*"

Question 14

Page 13, the vertical integrals can be written as $\int_{-H}^{0}$ rather than $\int_{-H(x)}^{0}$ since the bottom topography is flat.

Response:

Accepted.

Question 15

Page 13, at what time did the initial mode-2 ISW contain 146.2 KJm^{-1}? Just before the introduction of the shear?

Response:

Yes. The description of initial energy has been improved.

The related descriptions were added to the revision as follows (see also Page 17, Lines 10 – 12 in the main text):

"*The total energy of the initial mode-2 ISW just before the introduction of the shear calculated by the above expressions was 146.2 KJ* m^{-1},"

Question 16

Page 13, Define EOF and give a brief overview of its applicability here. Why is it applicable while normal mode decomposition is not?

Response:

A brief overview of EOF has been added. The normal mode decomposition is not suitable since the flow field in our simulations appears to be highly nonlinear in nature (*Venayagamoorthy* and *Fringer*, 2007).

The related descriptions were added to the revision as follows (see also Page 17 Line 24 – Page 18, Line 3 in the main text):

"*To understand better how the mode-2 ISW is modulated with the presence of shear current and to determine the nature of the whole wave system, the EOF (empirical orthogonal function) method was applied to the modal decomposition. EOF is commonly used for mode decomposition and space-time-distributed datasets examination in oceanography (Venayagamoorthy and Fringer, 2007). Especially with strong nonlinearity properties, where the traditional normal mode decomposition is*

not suitable (Venayagamoorthy and Fringer, 2007)"

Question 17

Can you explain the periodicity of figure 10 b? Why is it a function of distance and not time? What about the long time behaviour (when the wave approaches x = 0)?

Response:

We revised Figure 10 to give the variation with a function of time (Figure 7). The periodicity was caused by the superimposition of the energy of the mode-1 oscillating tail and the trailing mode-2 energy. These features trailed the mode-2 ISW with different wavelengths and therefore exhibited periodicity. The long-term behaviour of wave structure can be viewed in the response to major question 13.

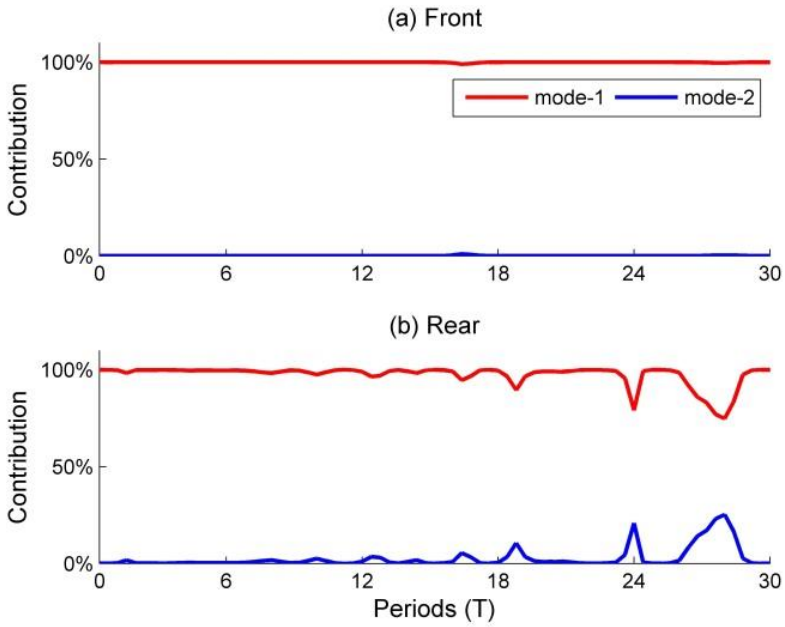

Figure 7. Percent contributions of mode-1 and mode-2 to the total kinetic energy in case ($\Delta = 0$) from 0 to 30 T at the (a) front and (b) rear of the mode-2 ISW.

Question 18

What are the breakdowns of the energy flux in terms of KEf , APEf , and W? What happens before t = 6T?

Response:

The breakdowns of the energy flux have been plotted accordingly (Figure 8), and we also refined Figure 11 in the previous manuscript to show the energy flux before 6 T. The pressure perturbation energy flux dominates the energy flux both in the front and rear, and this phenomenon accords with *Lamb* and *Nguyen* (2009). Before 6 T, the mode-2 ISW deformed due to the shear effect, and the forward-propagating long wave and amplitude-modulated wave packet were not generated completely yet.

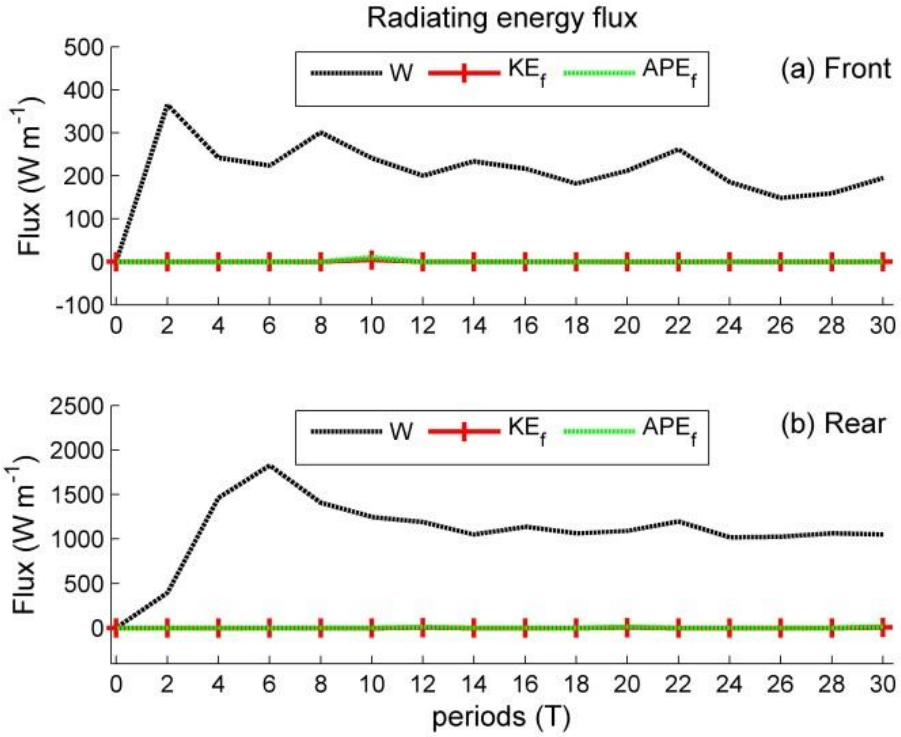

Figure 8. The breakdowns of the energy flux in terms of W, KE_f, and APE_f.

The related descriptions were added to the revision as follows (see also Page 20, Lines 7 – 10 in the main text):

"*The pressure perturbation generally make the largest instantaneous contributions to the total energy flux (Lamb and Nguyen, 2009; Venayagamoorthy and Fringer, 2007). For an ISW, the pressure perturbation term could be dominant (Lamb 2007). Since we focused on the energy loss of the mode-2 ISW, a total energy flux was analysed in the following paragraph.* "

Question 19

Page 15, lines 11-13. I'm still not convinced that the following is true: "the high radiating flux before 12 T indicates the generation process of the amplitude modulated wave packet and that the relative low radiating energy flux above 12 T is caused by the generation of an oscillating tail." The authors have yet to clearly show that the amplitude-modulated wave packet is short lived while the oscillating tail is persistent.

Response:

We plotted the energy flux in the rear of the mode-2 ISW induced by amplitude-modulated wave packet and oscillating tail, respectively (Figure 9). The amplitude-modulated wave packet has a relative high energy flux during the early stage of modulation, and an oscillating tail with a small energy flux appeared after 12 T.

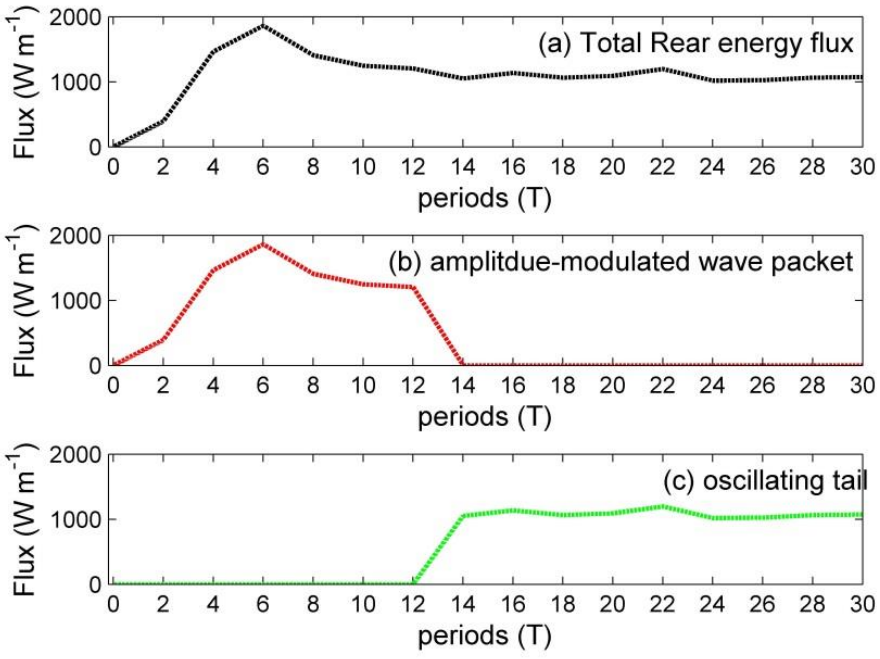

Figure 9. The total energy flux in the rear of the mode-2 ISW and the energy fluxes induced by the amplitude-modulated wave packet and oscillating tail.

Question 20

Page 16, line 13. It appears that the authors haven't been rigorous enough about how the energy is transferred. Why use the word 'suggests'?

Response:

This sentence has been refined accordingly.

The related descriptions were revised as follows (see also Page 21, Lines 10 – 13 in the main text):

"*Combining the results of the energy flux in front and rear of the mode-2 ISW (Fig. 13), thus, in the early stage of modulation, the amplitude-modulated wave packet could make a larger contribution to the energy transfer process.*"

Question 21

Table 2. Should the units be KW m^{-1}?

Response:

The units of energy loss rates were W m^{-1}, and it was in consistent with the observations (10 W m^{-1}) of *Shoyer* et al., (2010)

Question 22

Page 17, line 8. which observations where compared? and where? Were there more than the Shroyer et al. (2010) paper?

Response:

The initial expression has been improved. The wavelength and amplitude of the mode-2 ISW were chosen to match the observations in the New Jersey Shelf (*Shroyer* et al., 2010).

The related descriptions were added to the revision as follows (see also Page 23, Lines

1 – 2 in the main text):

"*The wavelengths and amplitudes of the mode-2 ISWs were selected to be comparable to the observation of Shroyer* et al. *(2010) on the New Jersey Shelf.*"

Question 23

Figure 15. What field is being plotted? Density? Which isopycnal is being plotted?

Response:

The mean density isopycnals of upper and lower layer were plotted, and the caption has been improved.

Question 24

The text at times is missing articles (such as 'the') and the tense is sometimes mixed up. Please review for grammar.

Response:

We have checked and improved the expressions of the manuscript. The NPG Language Editing service was contracted to review and polish the revised manuscript before the submission.

Reference

Grimshaw R. Wave action and wave-mean flow interaction, with application to stratified shear flows[J]. Annual Review of Fluid Mechanics, 16(1): 11-44, 1984.

Grimshaw R, Pelinovsky E, Talipova T. Modelling internal solitary waves in the coastal ocean[J]. Surveys in Geophysics, 28(4): 273-298, 2007.

Grimshaw R, Pelinovsky E, Taipova T, et al. Rogue internal waves in the ocean: long wave model[J]. The European Physical Journal Special Topics, 185(1): 195-208, 2010.

Grisouard, N., & Staquet, C. Numerical simulations of the local generation of internal solitary waves in the Bay of Biscay. Nonlin. Processes in Geophys., 17(5), 575-584, 2010.

Guo C, Chen X. Numerical investigation of large amplitude second mode internal solitary waves

over a slope-shelf topography[J]. Ocean Modelling, 2012, 42: 80-91, 2012.

Lamb K G. Energetics of internal solitary waves in a background sheared current[J]. Nonlinear Processes in Geophysics, 17(5): 553, 2010.

Lamb K G, Nguyen V T. Calculating energy flux in internal solitary waves with an application to reflectance[J]. Journal of Physical Oceanography, 39(3): 559-580, 2009.

Maderich V, Talipova T, Grimshaw R, et al. Interaction of a large amplitude interfacial solitary wave of depression with a bottom step[J]. Physics of Fluids, 22(7): 076602, 2010.

Stastna M, Lamb K G. Large fully nonlinear internal solitary waves: The effect of background current[J]. Physics of fluids, 14(9): 2987-2999, 2002.

Terletska K, Jung K T, Talipova T, et al. Internal breather-like wave generation by the second mode solitary wave interaction with a step[J]. Physics of Fluids, 28(11): 116602, 2016.

Venayagamoorthy S K, Fringer O B. On the formation and propagation of nonlinear internal boluses across a shelf break[J]. Journal of Fluid Mechanics, 577: 137-159, 2007.

Xie, J., He, Y., Chen, Z., Xu, J., & Cai, S. Simulations of internal solitary wave interactions with mesoscale eddies in the northeastern South China Sea. J.Phys. Oceanogr., 45(12), 2959-2978, 2015.

Yuan C, Grimshaw R, Johnson E. The evolution of second mode internal solitary waves over variable topography[J]. Journal of Fluid Mechanics, 836: 238-259, 2018.

Response to Reviewer 2:

General comment:

The effect of a background shear current on the evolution of a mode-2 internal solitary wave is investigated using the MITgcm numerical model. Three features were identified due to the modulation of the mode-2 wave by the background shear, namely, (i) forward-propagating long waves, (ii) an amplitude modulated wave packet behind the mode-2 wave and (iii) an oscillating tail. The distance between the centre of the shear layer and the centre of the pycnocline was varied such that the distance went in incremental values from zero (no offset) to offsets in which the centre of the shear layer was below that of the pycnocline. It was shown that the forward-propagating waves were insensitive to the offset distance while the oscillating tail and the wave packet decreased in their respective amplitudes as the offset was increased. Implications for energy transfer and energy depletion of the original mode-2 wave are discussed and comparison to a related field study (Shroyer et al. 2010) is given.

The paper is original and makes some interesting findings, as such I am in favor of publication but unfortunately the paper is not suitable in its present form. The following comments and suggestions are provided should the authors wish to rework the paper.

Response:

Thank you for your encouraging and constructive comments, which greatly contributed to improving the manuscript. We carefully read and considered the comments and made substantial revisions. We hope you find these revisions acceptable, and we highly appreciate your suggestions and comments. We highlight the main revisions in the manuscript, and the important points are described below.

Question 1

The paper is littered with grammatical and typographical errors. A thorough check is required.

Response:

We have checked and improved the expressions of the revised manuscript. The NPG Language Editing service was contracted to review and polish the revised manuscript before submission.

Question 2

Abstract lines 13-16 : this is not at all clear to the reader. The reader only knows what these features are AFTER reading the paper.

Response:

Thanks for your suggestion. The abstract has been rewritten and improved accordingly.

The related descriptions were revised in the revision as follows (see also Page 1, Lines 12 – 27 in the main text):

"*The evolution of mode-2 internal solitary waves (ISWs) modulated by background shear currents was investigated numerically. The mode-2 ISW was generated by "lock-release" method, and the background shear current was initialized after the mode-2 ISW became stable. Five sets experiments were conducted to assess the sensitivity of modulation process to the direction, polarity, magnitude, shear layer thickness and offset extent of background shear current. Three distinctly different shear-induced waves were identified as forward-propagating long wave, oscillating tail and amplitude-modulated wave packet in the presence of shear current. The amplitudes of forward-propagating long wave and amplitude-modulated wave packet are positively proportional to the magnitude of shear but inversely proportional to the thickness of shear layer, as well as the energy loss of mode-2 ISW during modulation. The oscillating tail and amplitude-modulated wave packet show symmetric variation when the background shear current is offset upward or downward, while the forward-propagating long wave was not. For comparison, one control experiment was configured according to the observations of Shroyer et al (2010), in first 30 periods, ~36% of total energy lost at an average rate of 9 W* m^{-1} *in the presence of shear*

current, it would deplete the energy of initial mode-2 ISWs in ~4.5 h, corresponding to a propagation distance of ~5 km, which is consistent with in situ data."

Question 3

Abstract: The definition of delta is not clear e.g. which distance (shear or pycnocline centre) is divided by which ?

Response:

The definition of Δ has been clarified.

The related descriptions were revised in the revision as follows (see also Page 5, Lines 7 - 9 in the main text):

"*The asymmetry parameter Δ is defined as follows:*

$\Delta = \frac{D_s - z_0}{h/2}$

where D_s denotes the depth of shear centre and h denotes the thickness of pycnocline."

Question 4

Abstract: long waves are said to be "robust" to delta. What does this mean? Insensitive ? Not affected by ?

Response:

'Insensitive' is more suitable, and the description has been changed accordingly.

The related descriptions were added to the revision as follows (see also Page 1, Lines 21 – 23 in the main text):

"*The oscillating tail and amplitude-modulated wave packet show symmetric variation when the background shear current is offset upward or downward, while the forward-propagating long wave was insensitive to it.*"

Question 5

Introduction: Mode-2 waves have also been remotely observed please see and reference JACKSON, CHRISTOPHER R., et al. "Nonlinear Internal Waves in Synthetic Aperture Radar Imagery." *Oceanography*, vol. 26, no. 2, 2013, pp. 68–79. *JSTOR*, JSTOR, www.jstor.org/stable/24862037.

Response:

Thank you for your suggestion. This reference has been included to provide evidence for the existence of mode-2 ISWs (see also Page 2, Line 5 in the revised manuscript).

Question 6

Introduction line 6: "in slope" not sure why the authors make specific reference to a slope here, e.g. can we infer that convex and concave are observed as much as one another in areas where there is not a slope ?

Response:

We revised this sentence following *Yang* et al. (2010) to clearly summarize the observation of mode-2 ISWs. As introduced by *Yang* et al. (2010), a concave slope is seldom observed because it requires a 'thick' middle layer, and this stratification is rare on the continental slope and shelf.

The related descriptions were added to the revision as follows (see also Page 2, Lines 9 – 10 in the main text):

"*In contrast, concave mode-2 ISWs are seldom observed because the stratification with a thick middle layer is rare (Yang* et al., *2010)*"

Question 7

P4 line 4 - define viscosities, what do the sub scripts stand for ?

Response:

We added the definition of viscosities in the revision. The subscripts '*v*' and '*h*' stand for 'vertical' and 'horizontal', respectively.

The related descriptions were added to the revision as follows (see also Page 4，Lines 9 - 10 in the main text):

"*The viscosity parameters were set to* 10^{-3} m^2s^{-1} *for the horizontal viscosity* v_H *and* 10^{-4} $m^2 s^{-1}$ *for the vertical viscosity* v_v *in the present study.*"

Question 8

P4 line 19 - it would be useful to have a figure here explaining exactly what Δ is. The authors may also like to consider adopting a similar definition and symbols to what others already use in the literature. For example see Neil Balmforth's work on identifying unstable modes in stratified flows.

Response:

We appreciate your constructive suggestion. We followed *Carpenter*, *Balmforth* and *Lawernce* (2010) to introduce the definition of an asymmetry parameter Δ to describe the asymmetry of the background shear current. We also improved Figure 2 in the revised manuscript to demonstrate the asymmetry parameter Δ.

Question 9

Figure 1: The authors have chosen to set the centre of the pycnocline at mid depth but in the field this is not the case and others (e.g Olsthoorn et al 2013 and Carr et al 2015) have shown that the location of the pycnocline relative to mid depth has a crucial influence on the shape and form of a mode-2 wave. This warrants discussion.

Response:

As suggested by *Olsthoorn* et al. (2013), the essential patterns of the mode-2 ISW generation processes are the same for both asymmetric and symmetric conditions,

suggesting that the basic structure of a mode-2 ISW with an offset pycnocline is similar to that for a mid-depth pycnocline. However, the asymmetric stratification can amplify the existing instability and induce asymmetrical instability (*Olsthoorn* et al., 2013), leading to more complicated circumstances, which makes it difficult to investigate the modulation process of mode-2 ISWs due to the presence of shear currents. To examine the influences of the background shear currents on the evolution process of a mode-2 ISW, a symmetric stratification was used in the present work following previous mode-2 works (*Terletska* et al., 2016; *Deepwell* and *Stastna*, 2016; *Deepwell* et al., 2017).

Question 10

Figure 2: The figure shows that the larger Δ is, the smaller Ri can be. This is interesting. Can the authors explain this finding ? Has it been reported elsewhere ? Eg Balmforth again.

Response:

As introduced by *Lamb* (2014), the Richardson number is defined as $Ri = N^2/u_z^2$, where N^2 is the buoyancy frequency and u_z is the shear. The shear remains unaffected to the position of the shear centre. In larger Δ cases, the shear centre was offset from the pycnocline centre. A relatively small N^2 appears at this location, but the shear remains unchanged, causing a smaller Ri.

A similar result was observed by *Lamb* and *Farmer* (2011). In their work, a smaller *Ri* number could be found when the shear centre was located farther from the centre of pycnocline. *Carpenter*, *Balmforth* and *Lawrence* (2010) repositioned the centre of pycnocline, and when the shear centre offset the pycnocline, a higher Richardson number appeared because of a larger buoyancy frequency.

Question 11

P 6 line 5. It is misleading to reference mode 1 work here as the initial condition (set

up behind the gate) is different and in fact it is the initial condition that is crucial in generating a mode-2 wave (as opposed to mode-1). It would be more appropriate to reference just Brandt & Shipley along with mode-2 papers such as Olsthoorn et al 2013 and/or Deepwell & Statsna 2016, and/or Statsna et al 2015.

Response:

Accepted. The citation has been modified.

The related descriptions were added to the revision as follows (see also Page 6, Lines 5 – 6 in the main text):

"*A rank-ordered mode-2 ISW train was generated by the "lock-release" method (Brandt and Shipley, 2014; Olsthoorn* et al.*, 2013; Deepwell and Stastna 2016; Stastna* et al.*, 2015).*"

Question 12

Figure 3: The authors have chosen to offset the shear centre downward of the pycnocline. Do they expect to see similar results (but symmetrically reversed) if it were to be offset in the upward direction? Presumably as the pycnocline centre is at mid-depth. What would happen however if the pycnocline centre were not at mid depth? Also the authors have chosen the shear such that the current in the top layer is in the same direction as the wave - this is similar to the overtaking cases in the work by Stastna et al 2015 and some comparison with that work should be given. Do the authors expect to see the same or different dynamics if the polarity of the shear current is reversed?

Response:

We improved and enriched the configuration of the experiment to generalize our research on the evolution of mode-2 ISWs in shear currents. We also added a comparison to *Stastna* et al. (2015) in the revision.

When the background shear current is shifted upward, the amplitude of the oscillating

tails and amplitude-modulated wave packet show nearly symmetrical variation trends compared to those with downward shifts. The amplitude of the forward-propagating long wave was insensitive to the offset of shear current (Figure 1 (a) and (b)). The energy losses of mode-2 ISW are also negatively proportional to the asymmetry parameter Δ in both upward and downward conditions (Figure 2(a) and (b)).

A polarity-reversal background shear current only reversed the polarity of the amplitude-modulated wave packet, oscillating tail and forward-propagating long wave.

Secondly, as we described in the response to Question 9, an asymmetric stratification can amplify existing instability and induce asymmetrical instability (*Olsthoorn* et al., 2010) as well as additional energy loss in mode-2 ISWs (*Carr* et al., 2015). Therefore, a higher energy loss rate is expected in the asymmetrical stratification.

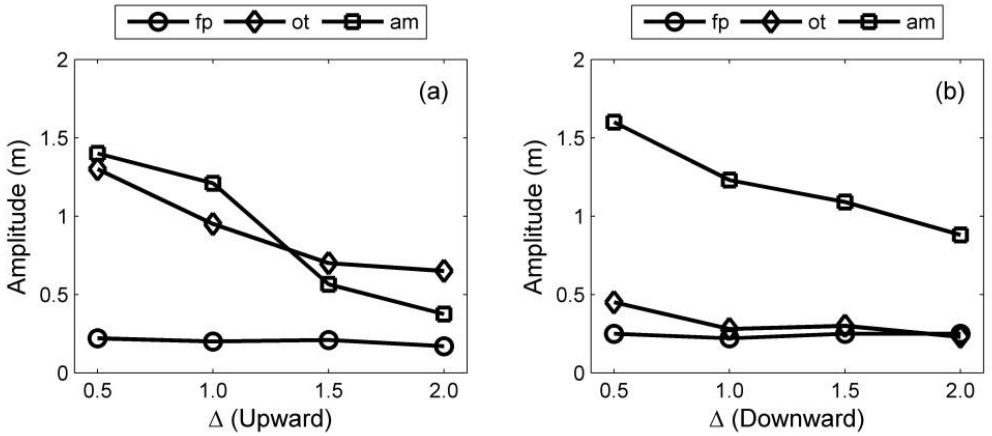

Figure 1. The summarized results of the amplitudes of the forward-propagating long wave (denoted by 'fp'), oscillating tail (denoted by 'ot') and amplitude-modulated wave packet (denoted by 'am') with the presence of (a) upward offset background shear currents at 30 T and (b) downward offset background shear currents at 30 T.

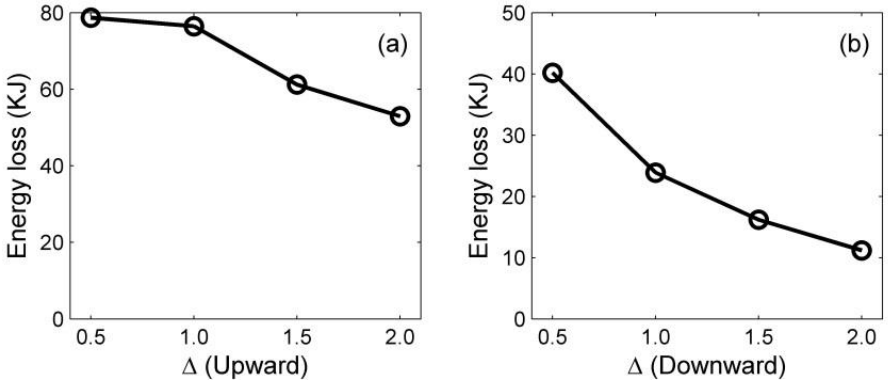

Figure 2. The summarized results of the energy loss of the mode-2 ISW at 30 T with the presence of (a) upward offset background shear currents and (b) downward offset background shear currents.

The related descriptions were added to the revision as follows (see also Page 13, Lines 22 – 27; Page 15, Line 27 – Page 16, Line 3; Page 23, Lines 13 – 18 in the main text):

"*In case P1, the polarity-reversal background shear current was initialized in the model. The properties of the wave structures in the case P1 and the control experiment were compared and no significant difference were found. Only the polarity of the forward-propagating long wave, oscillating tail and amplitude-modulated wave packet are reversed in case P1. This result indicates that the polarity of those shear-induced wave structures is closely related to the polarity of the background shear current.*"

"A similar variation trend could be found in the upward offset cases (Fig .10 (c)). The amplitudes of the oscillating tail and amplitude-modulated wave packet decreased monotonically as the shear current was offset upward. The forward-propagating long wave was barely affected by Δ and remained constant at approximately 0.2 m in all offset cases."

"*Stastna* et al. *(2015) investigated the mode-2 ISW interaction with mode-1 ISW at the same scale. The authors concluded that the shear current is vital, while the deformation of the pycnocline only slightly altered the structure of the mode-2 ISW. For our results, we focused on the effect of shear current, which could be induced by baroclinic eddies, baroclinic tides or wind. We found a deformation of mode-2 ISW and it illustrated asymmetry during the modulation in the presence of background shear current, it is coincident with the conclusion given by Stastna et al. (2015).*"

Question 13

P. 7 line 6 - it'd be useful if c_p were given and/or c presented in non-dimensional form.

Response:

The nondimensional form has been used in the revised paper (see also Page 8, Lines 4 - 7).

Question 14

Figure 4 caption: (a) “wave form” is this temperature ? What quantity and scale is the colour bar ?

Response:

The ‘wave form’ is the density field of the initial mode-2 ISW. The caption has been modified, and the quantity and scale were added.

Question 15

Page 9 text and figures - it is difficult to see the forward propagating waves - can this be improved ?

Response:

This figure has been re-plotted, and the corresponding description has been revised.

Question 16

Page 13 line 8 - what are x_r and x_l taken to be though ?

Response:

The definitions of x_l and x_r have been clarified. x_l and x_r are denoted as the left and right boundaries, respectively, where the available potential energy flux equals zero (*Lamb*, 2010).

The related descriptions were added to the revision as follows (see also Page 17, Lines 7 – 9 in the main text):

"x_r *and* x_l *are the boundary locations of the integration region, and x satisfies* $x_l \leq x \leq x_r$. *During the calculation of the wave energy,* x_r *and* x_l *are denoted as the left and right boundaries, respectively, where the available potential energy flux equals zero (Lamb, 2010)*"

Question 17

Page 14 line 19 - confusing grammar suggests mode-1 are also short lived

Response:

Improved.

The related descriptions were added to the revision as follows (see also Page 19, Lines 11 – 13 in the main text):

"*Modulated by the background shear current, the mode-2 ISW exhibits a highly dissipated nature, and the high energy loss rate is comparable to that of the longer mode-1 ISW (Lamb and Farmer, 2011; Shroyer* et al.*, 2010).*"

Question 18

Page 17 line 22 - are the authors referring to the field here or their simulations?

Response:

The references have been included to support our finding.

The related descriptions were added to the revision as follows (see also Page 24, Line 22 – Page 25, Line 3 in the main text):

"*The superposition of an initially stable shear current and the mode-2 ISW induced a low Ri region with a minimum value of less than 0.01 in our simulation, indicating a possible development of shear instability (Barad and Fringer, 2010).*"

Question 19

Figs 13 and 14 and related discussion. If shear instability is present would you not expect to see overturning isopycnals ?

Response:

A zoom-in plot of the density contour at 2.8 T for the control experiment (case O5, Δ = 0) is provided to show the overturning process (Figure 3). The region of interest corresponds to Figure 17 (b) in the revised manuscript, which is accompanied by low Ri values. We included this comment and plot in the revision.

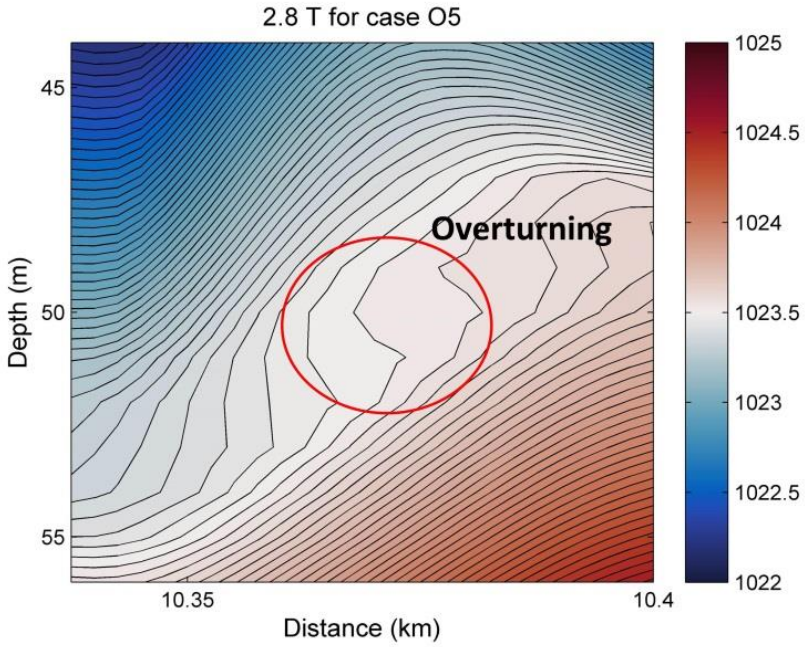

Figure 3. The density contour plot at 2.8 T for the control experiment (case O5).

The related descriptions were added to the revision as follows (see also Page 25, Lines 7 – 8 in the main text):

"The overturning process in the isopycnal could also be observed in the corresponding low Ri region (Fig. 18)."

Question 20

Page 19 Line 6 onward. Nice discussion which makes things a lot clearer for the reader, may be this should be given much earlier in the paper.

Response:

Thank you for your constructive suggestion. We have polished the structure of this paragraph and improved the description. It has been repositioned earlier in the revision. (See also Page 23, Line 19 – Page 24, Line 3 in the main text)

Question 21

Page 20 line 2. This is not clear - there was no background shear in the papers cited in line 1. What do the authors mean here by shear?

Response:

This sentence has been revised, and some closely related works have been cited.

The related descriptions were added to the revision as follows (see also Page 24, Lines 9 – 11 in the main text):

"*An oscillating tail induced by shear was also observed in similar studies (Carr* et al., *2011, Stamp and Jacka, 1995). The generation of this feature could be related to the shear, and the tail was sustained by continuous energy input.*"

Reference

Carpenter J R, Balmforth N J, Lawrence G A. Identifying unstable modes in stratified shear layers[J]. Physics of Fluids, 22(5): 054104, 2010.

Carr M, Davies P A, Hoebers R P. Experiments on the structure and stability of mode-2 internal solitary-like waves propagating on an offset pycnocline[J]. Physics of Fluids, 2015, 27(4): 046602.

Deepwell D, Stastna M. Mass transport by mode-2 internal solitary-like waves[J]. Physics of Fluids, 28(5): 056606, 2016.

Deepwell D, Stastna M, Carr M, et al. Interaction of a mode-2 internal solitary wave with narrow isolated topography[J]. Physics of Fluids, 29(7): 076601, 2017.

Lamb K G. Energetics of internal solitary waves in a background sheared current[J]. Nonlinear Processes in Geophysics, 17(5): 553, 2010.

Lamb K G. Internal wave breaking and dissipation mechanisms on the continental slope/shelf[J]. Annual Review of Fluid Mechanics, 46: 231-254, 2014.

Lamb K G, Farmer D. Instabilities in an internal solitary-like wave on the Oregon shelf[J]. Journal of Physical Oceanography, 41(1): 67-87, 2011.

Olsthoorn J, Baglaenko A, Stastna M. Analysis of asymmetries in propagating mode-2 waves[J]. Nonlinear Processes in Geophysics, 20(1): 59-69, 2013.

Stastna M, Olsthoorn J, Baglaenko A, et al. Strong mode-mode interactions in internal solitary-like waves[J]. Physics of Fluids, 27(4): 046604, 2015.

Terletska K, Jung K T, Talipova T, et al. Internal breather-like wave generation by the second mode solitary wave interaction with a step[J]. Physics of Fluids, 28(11): 116602, 2016.

Yang Y J, Fang Y C, Tang T Y, et al. Convex and concave types of second baroclinic mode internal solitary waves[J]. Nonlinear Processes in Geophysics, 17(6): 605, 2010.

Response to Reviewer 3:

General comment:

The evolution of the mode-2 internal solitary waves in fluid with stratification in density and shear flow is studied numerically with use MITgcm software. It is demonstrated that initial solitary wave disturbance splits on several wave groups: forwarding-propagated long waves, amplitude-modulated wave packet (which is identified as breather) and oscillating tail behind of soliton. Such groups attenuate with distance due to transfer processes, viscosity and shear instability. Interesting moment of this study is also the difference in the location of pycnocline and shear flow. Obtained results are important for understanding processes related with mode-2 internal waves and I may recommend publishing given paper.

Response:

Thank you very much for your constructive and helpful comments, which are highly valuable for us in improving the presentation and quality of the manuscript. We have carefully read the comments and made substantial revisions accordingly. We hope you find these revisions acceptable, and we greatly appreciate your suggestions and comments. We highlight the main revisions in the manuscript, and a point-to-point response is provided below.

Question 1

In fact, the difference between oscillating tail and amplitude-modulated packet (breather) is not clear visible. For instance, the modal structure is discussed on Fig. 10, but it will be more useful to see modal structure on waves for different times. The first mode contributes in energy mainly, but what is a difference in amplitudes of modes in the pycnocline?

Response:

The related figures have been improved to clearly demonstrate the structures of the oscillating tail and amplitude-modulated wave packet. The amplitude-modulated wave

packet appeared at the end of oscillating tail as steady-state envelopes *(Terletska* et al., 2016), and it could be clearly observed at the end of the oscillating tail (Figure 1). We have also added a plot to show the modal structures of waves for different times accordingly (Figure 2 and 3). Mode-1 shows the same depression or elevation on both sides of the pycnocline, while mode-2 exhibits a "concave" or "convex" nature, causing elevated and depressed amplitudes on both sides of the pycnocline simultaneously.

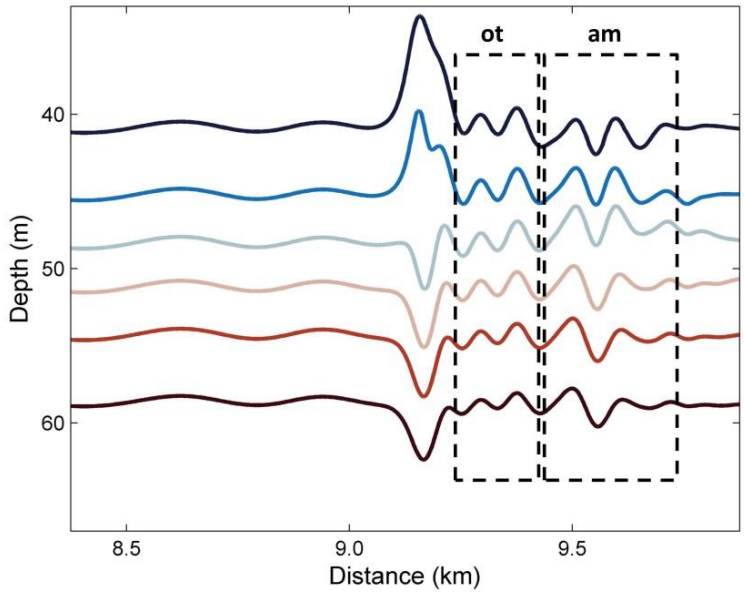

Figure 1. The evolution process of mode-2 ISW in case O5 at 14 T, where the 'ot' and 'am' denoted the oscillating tail and amplitude-modulated wave packet, respectively (see also FIigure 4(d) in the manuscript).

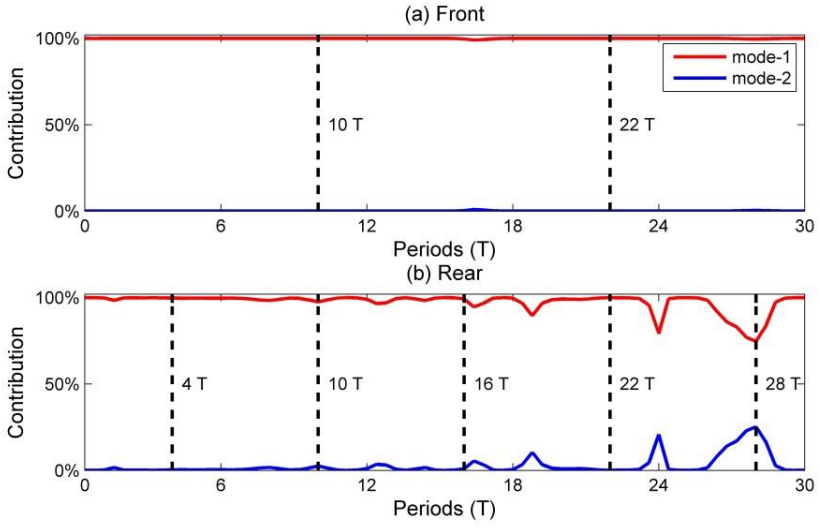

Figure 2. Percent contributions of mode-1 and mode-2 to the total kinetic energy in control experiment (case O5 with Δ = 0) from 0 to 30 T at the (a) front and (b) rear of the mode-2 ISW, the dash lines indicate the cross section where the model structures on waves shown in Figure 2.

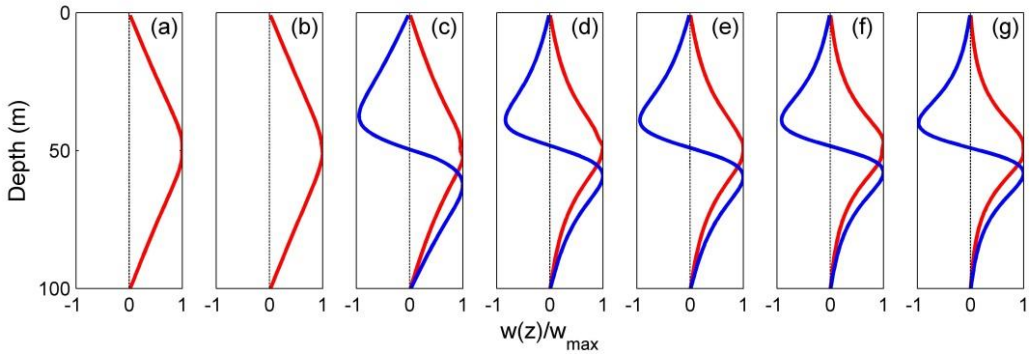

Figure 3. The model structures on mode-1 (red solid line) and mode-2 (blue solid line) waves in front of the mode-2 ISW at (a) 10 T, (b) 22 T and in rear of the mode-2 ISW at (c) 4 T, (d) 10 T, (e) 16 T, (f) 22 T and (g) 28 T for control experiment (case O5).

The related descriptions were added to the revision as follows (see also Page 18, Lines 13 – 18 in the main text):

"*The model structures of forward-propagating long wave for different times show its mode-1 nature was stable during the evolution of mode-2 ISW in the background shear current (Fig. 12 (a) and (b)). In the rear of the mode-2 ISW, the model structures of trailing waves transformed slightly with the time (Fig. 12 (c) – (g)), the wave-induced current are more and more concentrated around the pycnocline far away from the mode-2 ISW.*"

Question 2

What is an origin of the forward-propagating long waves? Are they generated in the initial time only?

Response:

The forward-propagating long wave was generated by the collapse of mixing induced by shear instability. This feature was generated persistently accordingly to the Hovmöller plot (Figure 4).

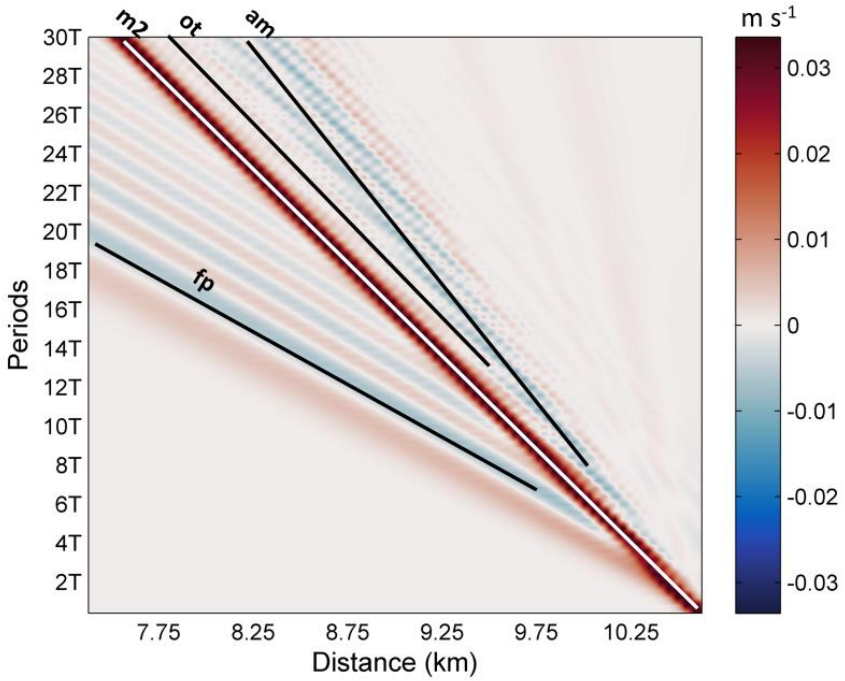

Figure 4. Hovmöller plot of horizontal velocity without background shear current at the surface. The mode-2 ISW, forward-propagating long wave, oscillating tail and amplitude-modulated wave packet are denoted by 'm2', 'fp', 'ot' and 'am', respectively. The color bar ranges from -0.034 to 0.034 m/s.

The related descriptions were added to the revision as follows (see also Page 10, Lines 13 - 15; Page 24, Lines 13 - 15 in the main text):

"*A Hovmöller plot (Fig. 6) of horizontal velocity without the background shear current at the surface was plotted. The forward-propagating long wave, oscillating tail and amplitude-modulated wave packet were found to propagate persistently.*"

"*Forward-propagating long waves were also observed by Yuan* et al. *(2018), who found that some small but significant long wavelength mode-1 waves appeared ahead of mode-2 ISWs. The forward-propagating long wave was generated by the collapse of mixing induced by shear instability.*"

Question 3

Usually oscillatory tail is generated behind solitary wave due to dissipation, and its energy is increased when soliton energy is decreased. Is it observed in numerical

simulations?

Response:

The total energy of the mode-2 ISW and the oscillating tail in numerical simulation was calculated (Figure 5). After the generation of the oscillating tail, its energy increased, while the total energy of the mode-2 ISW decreased.

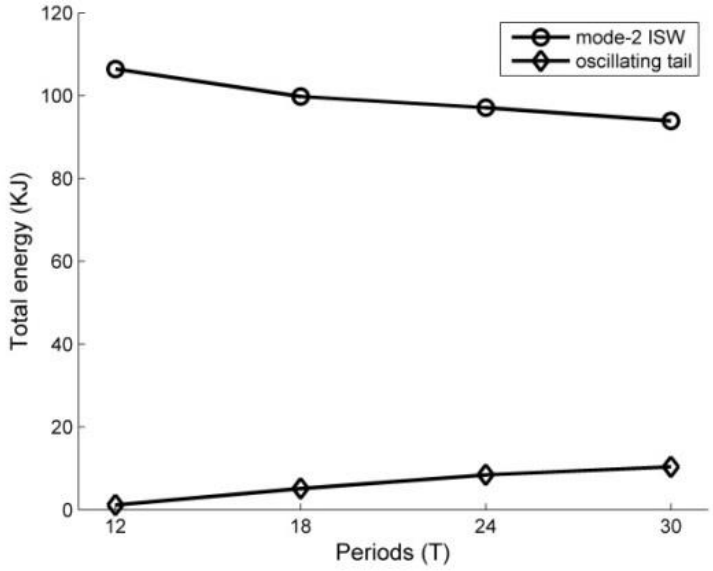

Figure 5. The total energy of the mode-2 ISW and oscillating tail in different periods.

Technical comments:

Question 1

Axis z is directed up. Looking on formulas (1) and (2) z = 0 corresponds to the fluid surface, but on Fig. 3 – to the fluid bottom.

Response:

Corrected.

Question 2

Fig. 6. There is no vorticity scale.

Response:

Added.

Reference

Terletska K, Jung K T, Talipova T, et al. Internal breather-like wave generation by the second mode solitary wave interaction with a step[J]. Physics of Fluids, 28(11): 116602, 2016.

The evolution of mode-2 internal solitary waves modulated by background shear currents

Peiwen Zhang [1, 3], Zhenhua Xu [1, 2, 3*], Qun Li [4*], Baoshu Yin [1, 2, 3], Yijun Hou[1, 2, 3], Antony K. Liu[5]

[1]Key Laboratory of Ocean Circulation and Waves, Institute of Oceanology, Chinese Academy of Sciences, Qingdao, 266071, China.

[2]Qingdao National Laboratory for Marine Science and Technology, Qingdao, 266071, China.

[3]University of the Chinese Academy of Sciences, Beijing, 100049, China.

[4]Polar Research Institute of China, Shanghai, 200136, China.

[5]Ocean University of China, Qingdao, 266100, China.

Correspondence to: Zhenhua Xu (xuzhenhua@qdio.ac.cn); Qun Li (liqun@pric.org.cn)

Abstract. The evolution process of mode-2 internal solitary waves (ISWs) modulated by the background shear currents was investigated numerically. The mode-2 ISW was generated by "lock-release" method, and the background shear current was initialized after the mode-2 ISW became stable. Five sets experiments were conducted to assess the sensitivity of modulation process to the direction, polarity, magnitude, shear layer thickness and offset extent of background shear current. Three distinctly different shear-induced waves were identified as forward-propagating long wave, oscillating tail and amplitude-modulated wave packet in the presence of shear current. The amplitudes of forward-propagating long wave and amplitude-modulated wave packet are positively proportional to the magnitude of shear but inversely proportional to the thickness of shear layer, as well as the energy loss of mode-2 ISW during modulation. The oscillating tail and amplitude-modulated wave packet show symmetric variation when the background shear current is offset upward or downward, while the forward-propagating long wave was insensitive to it. For comparison, one control experiment was configured according to the observations of Shroyer et al (2010),~~The forward propagating long wave, amplitude modulated wave packet were generated during the early stage of modulation, where the amplitude modulated wave packet were suggested playing an important role in the energy transfer process, and then the oscillating tail was generated and followed the solitary wave. Five different cases were introduced to assess the sensitivity of the energy transfer process to the Δ, which defined as a dimensionless distance between the centers of pycnocline and shear current. The forward propagating long waves were found robust to the Δ, but the oscillating tail and amplitude modulated wave packet~~

~~decreased in amplitude with increasing Δ. The highest energy loss rate was observed when Δ = 0. I~~in first 30 periods, ~36% of the total energy lost at an average rate of 9 W m^{-1}, it would deplete the energy of the solitary wave in ~4.5 h, corresponding to a propagation distance of ~5 km, which is consistent with with in situ data~~the hypothesis of *Shroyer et al.* (2010), who speculated that the mode-2 ISWs are "short-lived" in the presence of shear currents~~.

1 Introduction

Internal solitary waves (ISWs) are commonly observed in stratified oceans, especially in coastal and continental shelf regions (Grimshaw et al., 2010； Helfrich and Melville, 2006; Lamb, 2014). While mode-1 ISWs are frequently observed by in situ observations (Farmer et al., 2009; Klymak and Moum, 2003; Moum et al., 2006) and by remote sensing (Liu et al., 1998; Liu et al., 2004; Zhao et al., 2004; Zhao and Alford, 2006), higher modes are relatively rare captured (Jackson et al., 2013). Even so, with the improvement of observation, mode-2 ISWs have been reported recently (Liu et al., 2013; Shroyer et al., 2010; Yang et al., 2009; Yang et al., 2010). Most of previously reported mode-2 ISWs were categorized as convex types, which have the potential to transport mass (Brandt and Shipley, 2014; Deepwell and Stastna, 2016; Salloum et al., 2012). In contrast, concave mode-2 ISWs are seldom observed because the stratification with a thick middle layer is rare (Yang et al., 2010).~~In contrast, concave mode-2 ISWs are not as frequently observed in slope areas as convex types. Yang et al. (2010) suggested that the occurrence of concave mode-2 ISWs requires the presence of a thick pycnocline, which is rarely present in a shallow sea.~~

Majority of studies of mode-2 ISWs aimed at interpreting their generation mechanisms under different conditions (Helfrich and Melville, 1986; Huttemann and Hutter, 2001; Stastna and Peltier, 2005; Vlasenko et al., 2010). ~~Yuan et al. (2018) investigated the propagation of mode-2 ISWs over slope-shelf topography, suggesting the propagation manner of mode-2 ISWs over a slope is similar to the mode-1 ISW, but presenting a rather complex wave field.~~ Under most circumstances, mode-2 ISWs show the specific phenomenon of a "short-lived" nature (Ramp et al., 2012; Shroyer et al., 2010; Yang et al., 2010). Ramp et al. (2012) concluded that mode-2 ISWs around the Heng-Chun Ridge would dissipate in 8.9 hours, suggesting mode-2 ISWs are highly dissipative when traveling around rough topographical features. ~~Stastna et al. (2015) investigated the strong interaction between mode-1 and~~

~~mode-2 ISWs, illustrating the mode-2 ISWs deformed significantly and became ephemeral during the interaction.~~ Terletska et al. (2016) showed the decaying of mode-2 ISWs was induced by a step-like topography. The forward-propagating long waves, breather-like internal waves (BLIWs) and an oscillating tail were generated during the adjustment process. Yuan et al. (2018) observed the existence of a long mode-1 wave ahead of mode-2 ISW during the evolution of mode-2 ISW over variable topography and found that this process cannot be characterized by KdV theory. The authors suggested using the MITgcm model, which can solve all modes to investigate the integrated evolution process of mode-2 ISWs in variable background conditions.

The ephemeral phenomenon of mode-2 ISWs could also be induced by the background shear currents. They are more common in the open ocean because they can be induced by the baroclinic eddies, baroclinic tides, wind and internal solitary wave (Chen et al., 2011; Wang et al., 1991; Xu et al., 2013; Xu et al., 2016; Stastna et al, 2015). The evolution of mode-1 ISWs in background shear current was extensively studied (Stastna and Lamb, 2002, Lamb, 2010, Grimshaw et al., 2007, Fructus et al., 2009). Lamb (2010) investigated the energetics of mode-1 ISWs in a background shear current, providing some methods commonly used to calculate the energy under that circumstance. Stastna and Lamb (2002) considered the effects of background current on mode-1 ISWs and discussed the properties of ISWs during the breaking process. In comparison, few works on mode-2 ISW in shear flow have been produced. Vlasenko et al. (2010) observed mode-2 ISW followed by short wavelength mode-1 oscillating tail in the Luzon Strait. Liu et al. (2013) investigated the generation and evolution of mode-2 ISW in the South China Sea and concluded that the more dispersive mode-2 ISW might not propagate, evolve and persist for long time on the shelf. ~~In cases with large-scale currents, such as those induced by the wind and internal tides, the background currents should be present before the generation of the mode-2 ISW. Additionally, this circumstance is also possible in the presence of small-scale background currents and was observed by Orr and Evans (2015) over the New Jersey Shelf, which is near the field site of Shroyer et al. (2010). The steepening of internal tides generates both mode-1 and mode-2 ISWs on the New Jersey Shelf, and the mode-1 wave, which has a faster propagation speed, can overtake the mode-2 wave generated in the last period of the internal tide (Orr and Evans, 2015).~~

~~Previous~~ Their works focused on the shoaling pycnocline and topography, which were suggest to cause the ephemeral mode-2 ISWs, but the effects of background shear currents were neglected. Shroyer et al. (2010) was the sole one recording an integrated evolution process of mode-2 ISW and found that

leading mode-2 wave quickly deformed and developed a tail of short, small-amplitude mode-1 wave in the presence of background shear current. ~~Given the background conditions described by Shroyer et al. (2010), the stratification remains stable with a flat bottom, but the presence of background shear current could modulate the mode-2 ISW.~~ Therefore, the authors speculated that the background shear currents could produce instabilities and lead to the adjustment of ISWs and they also concluded that the wave-localized turbulence dissipation was comparable with that induced by mode-1 ISWs. Motivated by the results of Shroyer et al. (2010), in the present study, we numerically investigated the effect of shear currents on evolution process of mode-2 ISWs.~~we investigated the influence of shear currents on the mode-2 ISWs and presented the evolution processes and energy of mode-2 ISWs using numerical simulations~~. To reveal the sensitivity of the evolution of mode-2 ISWs to variable parameters of background shear currents, we introduced five sets of experiments (21 experiments in total) to generalize our research, including the magnitude, thickness of the shear layer, direction and offset (center of the shear layer relative to the center of the pycnocline) of the background shear current. ~~Five different cases were introduced to investigate the propagation of mode-2 ISWs in the presence of shear currents, since the background shear currents could symmetric around the center of the pycnocline or deviate for a distance from it.~~ These conditions are common in the oceans, for example, the internal tidal wave could be symmetric around the pycnocline (Duda et al., 2004), but in the shelf-slope area, the surface-intensified flow driven by wind could deviate for a distance from the center of pycnocline (Van de Boon, 2011).

The remainder of the paper is organized as follows: The numerical model configurations and background conditions are detailed in Sect. 2. In Sect. 3, the modulation process of mode-2 ISW in background shear currents and its sensitivity to varied background shear currents are presented and assessed. The decaying of mode-2 ISWs' energy and the effect of varied background shear current on it are analyzed and summarized in Sect. 4. In Sect. 5, details of mode-2 ISW evolution and characteristics of shear-induced waves are compared and discussed. Then, the results are summarized in Sect. 6.

~~The paper is organized as follows: The numerical model configurations and background conditions are detailed in Sect. 2. In Sect. 3, the results are presented and examined. The energy transfer process and the decaying of the mode-2 ISWs are analyzed in Sect. 4. In Sect. 5, details of mode-2 ISW evolution are discussed and compared. Then, the results are summarized in Sect. 6.~~

2 Numerical model and background condition

2.1 Model configuration

Our numerical simulations are based on the Massachusetts Institute of Technology general circulation model (MITgcm, Marshall et al., 1997). The nonhydrostatic capability of the MITgcm is turned on because ISWs represent a balance of nonlinearities and dispersions, with the latter derived from nonhydrostatic pressure.

A series of 2D numerical simulations were performed to investigate the evolution of mode-2 ISWs in the presence of background shear currents. The experimental domain was 12.8 km long and 100 m deep. The horizontal and vertical resolutions were 2.5 m with 5120 grids points and 0.5 m with 200 grid points, respectively. The time step was 0.4s in order to ensure that the Courant-Friedrichs-Lewy (CFL) condition was satisfied and the model was stable. The viscosity parameters were set to 10^{-3} m^2s^{-1} for the horizontal viscosity~~for~~ v_H and 10^{-4} $m^2 s^{-1}$ for the vertical viscosity~~for~~ v_v in the present study. The flux-limiting advection scheme for the tracers introduces numerical diffusivity which is needed for stability, so the explicit diffusivity was set to zero (Legg and Adcroft, 2003, Legg and Huijts, 2006, Legg and Klymak, 2008).

2.2 Stratification and background conditions

The choice of background density stratification in all experiments and the shear current in control experiment (case O5) followed the field observation over the New Jersey Shelf (Shroyer et al., 2010).~~The choice of background density stratification and shear currents followed the field observations over the New Jersey shelf (Shroyer et al., 2010).~~ The background stratification and shear currents adopted the hyperbolic tangent function for smoothing, which can be written as follows:

$$\rho(z) = \rho_0 - \frac{\Delta\rho}{2} tanh\left[\frac{(z+z_0)}{h}\right], \quad (1)$$

where $\rho_0 \equiv (\rho_1 + \rho_2)/2$ is the mean density of the vertical water column and $\Delta\rho \equiv (\rho_2 - \rho_1)$ is the difference in density between the upper layer ρ_1 (1022 kg m^{-3}) and bottom layer ρ_2 (1026 kg m^{-3})~~between the upper layer ρ_1 and bottom layer ρ_2~~. The h is the pycnocline thickness and z_0 is the depth of the pycnocline center. The function of background shear current is given by

$$U(z) = U_0 - \frac{\Delta U}{2} tanh\left[\frac{(z+D_s)}{h_s}\right], \quad (2)$$

where $U_0 \equiv (U_1 + U_2)/2$ is the mean background velocity of water column and $\Delta U \equiv (U_2 - U_1)$ is

the difference in background horizontal velocity between the upper layer U_1 and bottom layer U_2, and h_s is the thickness of shear layer.

In sensitive experiments, the magnitude of the shear current is denoted by U_d and defined as $|\Delta U|$. This value was varied from 0.5 U_d to 2.5 U_d in sensitivity test. Similarly, the thickness of shear layer was varied from 0.5 h_s to 2.5 h_s. In cases D1 and P1, an opposing and polarity-reversal background shear currents were initialized for examination, respectively. We further introduced an asymmetry parameter Δ to investigate the evolution of mode-2 ISWs in offset background shear current (Carpenter et al., 2010). The asymmetry parameter Δ is defined as follows:

$$\Delta = \frac{D_s - z_0}{h/2} \quad (3)$$

where D_s denotes the depth of shear centre and h denotes the thickness of pycnocline. Δ was varied from -2 to 2 (case O1 to case O9) to investigate the evolution of the mode-2 ISW in the offset background shear current.~~To reveal the sensitivity of energy transfer process to the relative locations of the pycnocline and background shear current, we introduced a dimensionless value Δ, which was defined as the distance between the centers of pycnocline and shear current nondimensionalized by the h/2, and the D_s indicates the center depths of the shear currents for five cases with different Δ.~~ The vertical distributions of the background shear currents, density and buoyancy frequency are shown in Fig. 1, and the detailed values for background stratification and currents in the present study are given in Table 1.

In all cases, the Richardson number of background current were estimated to be larger than 0.25, indicating the stable state of background environment.

~~In all five cases, the Richardson number were estimated to be larger than 0.25, indicating the stable state of the background environment (Fig. 2).~~

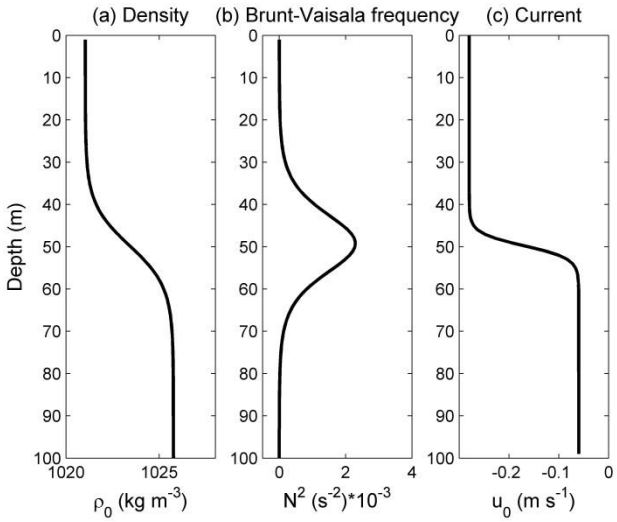

Figure 1. Vertical profiles of the (a) density, (b) buoyancy frequency and (c) background velocities in the control experiment (case O5).

~~**Figure 1:** Vertical profiles of the (a) density, (b) buoyancy frequency and (c) background velocities in the simulations, which includes the Δ = 0 (case 1), Δ = 0.5 (case 2), Δ = 1.0 (case 3), Δ = 1.5 (case 4) and Δ = 2.0 (case 5) marked by the cyan, blue, green, red, and black lines, respectively.~~

Table 1. Summary of parameters of variable background shear currents. The depth and thickness of the pycnocline are denoted by z_0 and h. The thickness of the shear layer is denoted by h_s, and the offset cases are indicated by asymmetry parameter Δ. The magnitude of the shear current is denoted by U_d. *Por* indicates the polarity of the background shear current, and "+" means a polarity-reversal shear current. The orientation of the background shear current is indicated by *Ori*, and "+" means an opposing shear current.

Case	z_0	h	h_s	Δ	U_d	*Por*	*Ori*
O1	50	10	3	-2	0.22	(-)	(-)
O2	50	10	3	-1.5	0.22	(-)	(-)
O3	50	10	3	-1	0.22	(-)	(-)
O4	50	10	3	-1.5	0.22	(-)	(-)
O5	50	10	3	0	0.22	(-)	(-)
O6	50	10	3	0.5	0.22	(-)	(-)
O7	50	10	3	1	0.22	(-)	(-)
O8	50	10	3	1.5	0.22	(-)	(-)
O9	50	10	3	2	0.22	(-)	(-)
H1	50	10	1.5	0	0.22	(-)	(-)

H2 (O5)	50	10	3	0	0.22	(-)	(-)
H3	50	10	4.5	0	0.22	(-)	(-)
H4	50	10	6	0	0.22	(-)	(-)
H5	50	10	7.5	0	0.22	(-)	(-)
U1	50	10	3	0	0.11	(-)	(-)
U2 (O5)	50	10	3	0	0.22	(-)	(-)
U3	50	10	3	0	0.33	(-)	(-)
U4	50	10	3	0	0.44	(-)	(-)
U5	50	10	3	0	0.55	(-)	(-)
D1	50	10	3	0	0.22	(-)	(+)
P1	50	10	3	0	0.22	(+)	(-)

Table 1: The parameter values for the initial background conditions

Parameters	**Values**
ρ_1	1026 kg m^{-3}
ρ_2	1022 kg m^{-3}
h	10 m
z_0	50 m
U_1	-0.28 m s^{-1}
U_2	-0.06 m s^{-1}
h_s	3 m
D_s (Δ = 0, 0.5, 1.0, 1.5, 2.0)	50, 52.5, 55, 57.5, and 60 m

Figure 2: Richardson numbers of the background state for the five cases with the Δ = 0, 0.5, 1.0, 1.5 and 2.0 marked by the cyan, blue, green, red, and black lines, respectively.

2.3 Modal initialization

A rank-ordered mode-2 ISW train was generated by the "lock-release" method without background current. (Brandt and Shipley, 2014; Olsthoorn et al., 2013; Deepwell and Stastna 2016; Stastna et al., 2015). Figure 3 demonstrate a schematic diagram of initialization process and the configuration of

model parameters. A mixed region was set to be symmetric around the centerline of the pycnocline at the right end, and its length l_{mix} and height h_{mix} were 375 m and 25 m, respectively.~~Rank-ordered mode-2 ISW train was generated by the "lock-release" method (Brandt and Shipley, 2014; Helfrich et al., 2010; Sutherland et al., 2013). Figure 3 demonstrates the configurations of the simulation domains. A mixed region was set symmetric around the centerline of the pycnocline at the right end, with a length of 375 m and height of 25 m.~~ The pycnocline was 10 m thick, and this dimension was indicated by *h*. the model was initialized at t = 0 s, and the rank-ordered mode-2 wave train emerged at t = 4000 s and propagated to the left of the domain, as shown in Fig. ~~3~~2, the leading mode-2 wave is extracted at that time and then propagated for 2000 s until it stabilized. The amplitude *A* of mode-2 ISWs was defined as the maximum displacement of the upper and lower isopycnals, which are equal in the initial state (Terletska et al., 2016). The wavelength *L* was defined as the width of the wave at half of the amplitude of the mode-2 ISW in the initial state. At 6000 s after the initialization of numerical model, the velocity field of background shear current was superimposed on the model.~~A is the amplitude of mode-2 ISW, and the wavelength *L* was defined as the width of the wave at half the amplitude. At 6000 s after the initialization of numerical model, the background shear currents were initialized in experiment.~~

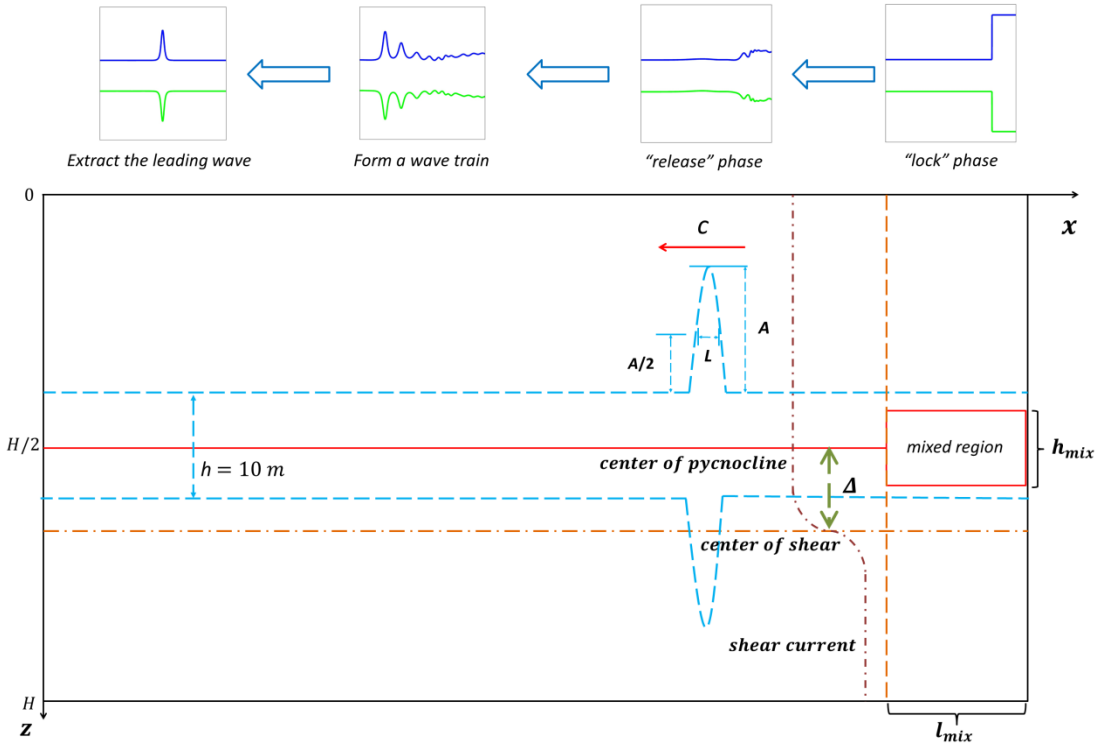

Figure 2. Schematic diagram of the modal configuration and initialization, where Δ denotes the asymmetry parameter, h denotes the thickness of pycnocline, c, A, and L indicated the propagation speed, amplitude and the wavelength of mode-2 ISW, h_{mix} and l_{mix} denote the height and length of mixed region, and H indicates the depth.

~~**Figure 3:** Schematic diagram of the modal configuration and initialization.~~

3 Results

3.1 Characteristics of mode-2 ISWs

The characteristics of initial mode-2 ISW were compared with KdV theory (Grimshaw et al., 2010). The vorticity and density fields of the leading single wave of a mode 2 ISW in the absence of the background shear current are shown in Fig. 3, and the wave exhibits a notably symmetric structure.~~The vorticity and temperature fields of the leading single wave of a mode-2 ISW in the absence of the background shear current are shown in Fig. 4.~~ The ISW had amplitude of 7 m, wave length of 62.5 m with a propagation speed at ~0.31 m s^{-1}, which was defined as c. It is slightly larger than the linear long-wave phase speed c_p (0.295 m s^{-1}) calculated by Taylor-Goldstein equation (Vlasenko et al., 2010) and nondimensionalized by long-wave phase speed as 1.05.~~It is slightly larger than the linear long wave phase speed c_p calculated by the Taylor-Goldstein equation (Vlasenko et al., 2010).~~ The typical time scale T for mode-2 ISW is 200 s which was calculated by L/c~~,~~. The modeled profile of the mode-2 wave is consistent with the theoretical solution of mode-2 ISW in the framework of KdV equation (white line in Fig. 3).~~and the wave exhibits a notably symmetric structure without mode-1 wave tail. As such, the mode-2 ISW remains stable and has the potential to propagate over a long distance. This finding is confirmed by the vorticity field shown in Fig. 4(b), which shows a stable and symmetric vortex dipole.~~

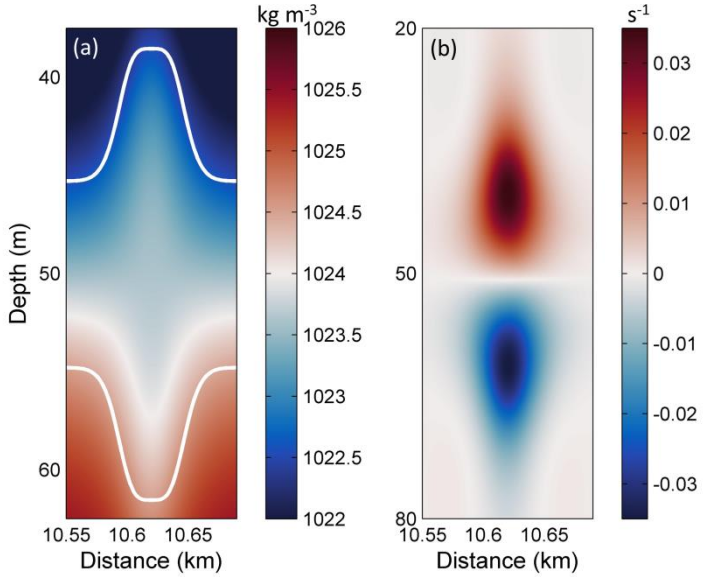

Figure 3. The characteristics of a single mode-2 ISW's (a) density field and (b) vorticity in the absence of background shear current. The white lines in (a) demonstrate the theoretical solution of mode-2 ISW in KdV framework.

~~**Figure 4:** The characteristics of a single mode-2 ISW's (a) wave form and (b) vorticity in the absence of background shear current.~~

3.2 The evolution of mode-2 ISW in in control experiment~~case 1~~

The evolution of a mode-2 ISW modulated by background shear current in control experiment (case O5) is shown in Fig. 4, with its corresponding vorticity field shown in Fig. 5.~~The evolution of a mode-2 ISW modulated by the background shear current in case 1 ($\Delta = 0$) is shown in Fig. 5, with its corresponding vorticity field shown in Fig. 6.~~ The mode-2 ISW was symmetric about the pycnocline center and the vorticity of the upper and lower parts counterbalance each other, demonstrating a dipole structure (Fig. 4 (a) and Fig. 5 (a)). ~~in the initial state (Fig. 5 (a) and Fig. 6 (a)).~~

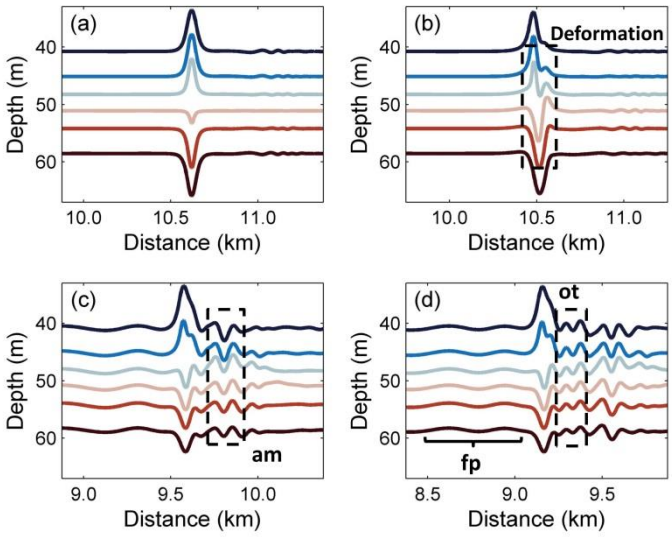

Figure 4. The evolution process of the mode-2 ISW in the case O5 (Δ = 0) for the different times (a) 0T, (b) 1.2T, (c) 10T, (d) 14T, where 'am', 'fp' and 'ot' denote the amplitude-modulated wave packet, forward-propagating long wave and oscillating tail, respectively.

~~**Figure 5:** The evolution process of the mode-2 ISW in the case 1 (Δ = 0) for the different times (a) 0T, (b) 1.2T, (c) 10T, (d) 14T.~~

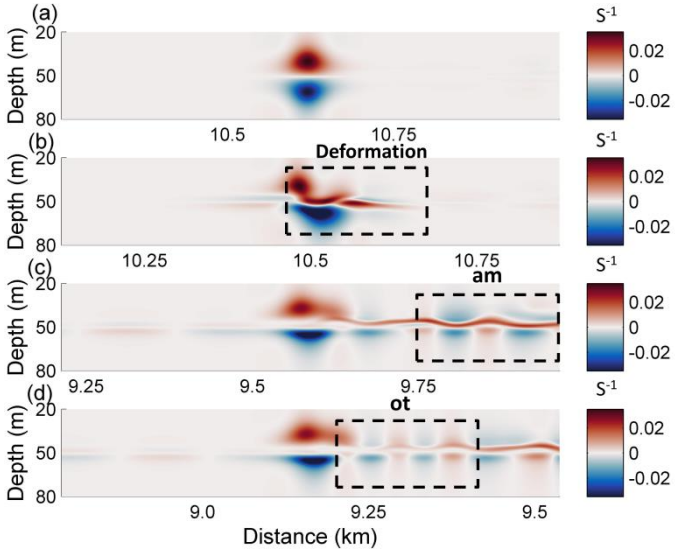

Figure 5. The evolution process of the vorticity field (s^{-1}) in the case O5 (Δ = 0) for the different times (a) 0T, (b)1.2T, (c) 10T, (d) 14T, where 'am', 'fp' and 'ot' denote the amplitude-modulated wave packet, forward-propagating long wave and oscillating tail, respectively.

~~**Figure 6:** The evolutiona process of the vorticity field in the case 1 (Δ = 0)for the different times (a) 0T, (b)1.2T, (c) 10T, (d) 14T.~~

Then, at 1.2 T after the ~~initialization~~ presence of background shear current, as shown in Fig. ~~6~~ 5 (b), the

shear led to the deformation of the dipole, with the upper part being pushed forward. It also caused the asymmetrical distribution of the vorticity in horizontal, which is associated with the generation of forward-propagating long waves and amplitude-modulated wave packet (Fig. ~~5~~ 4 (b)~~)~~), and the latter was defined as a pulsating wave packet (Clarke et al., 2000). The pulsating wave packet propagated with a steady-state envelope, inside which the waves oscillate freely with different amplitudes (Terletska et al., 2016). ~~In~~ To the aft of the ISW, ~~The~~ the shear induced by the background currents lead to the deformation of the vortex dipole, and an increasing complexity of the vorticity field implied intensive adjustment occurred.~~more energy is transferred from mode-2 ISWs to other wave forms~~. As illustrated in Fig. ~~6~~ 5 (c), ~~10 T after the initialization of background shear current,~~ the vorticity of the mode-2 ISW is redistributed to adapt to the background condition at 10 T. In that process, the vortex of the ISW shrank with the generation of an amplitude-modulated wave packet and a forward-propagating long wave. The amplitudes of shear-induced waves were defined as maximum isopycnal displacement (Stastna and Lamb, 2002).~~, which is related to the generation of an amplitude modulated wave packet and a forward propagating long wave, some of the energy of the ISW was transferred to them, and consequently, the vortex of the ISW shrank.~~ The forward-propagating long wave and amplitude-modulated wave packet can be seen in Fig. ~~5~~ 4 (c), with amplitudes of 0.25 m and 1.8 m respectively, and the latter was clearly observed at the rear of the mode-2 ISW.~~implying the amplitude modulated wave packet is more energetic.~~

The oscillating tail caused by the shear was visible between the mode-2 ISW and amplitude-modulated wave packet (Fig. ~~5~~ 4 (d)) at 14 T~~ after the initialization of background shear current~~, and it was a radiated mode-1 oscillatory disturbance trailing mode-2 ISW (Stamp and Jacka, 1995). A Hovmöller plot (Fig. 6) of horizontal velocity without the background shear current at the surface was plotted. The forward-propagating long wave, oscillating tail and amplitude-modulated wave packet were found to propagate persistently. The amplitude-modulated wave packet propagated independently from the ISW, indicating that it generated transiently.~~ The amplitude modulated wave packet propagated independently from the ISW, indicating that they were no longer related to the energy transfer of the mode-2 ISW.~~ Based on the vorticity field shown in Fig. ~~6~~ 5 (d) and the time-space varying nature (Fig. 6),~~,~~ the generation of the oscillating tail and the forward-propagating long wave was continuously sustained by the energy of the ISW. Therefore, they have the potential to drain the energy from an ISW over a long time scale. It should be noted that the forward-propagating long wave and

amplitude-modulated wave packet generated simultaneously, while the oscillating tail appeared after the amplitude-modulated wave packet propagated away from the mode-2 ISW.~~that the forward-propagating long wave formed when the background shear current is present.~~ Thus, the energy loss of the ISW caused by forward-propagating long waves occurs earlier than oscillating tail.

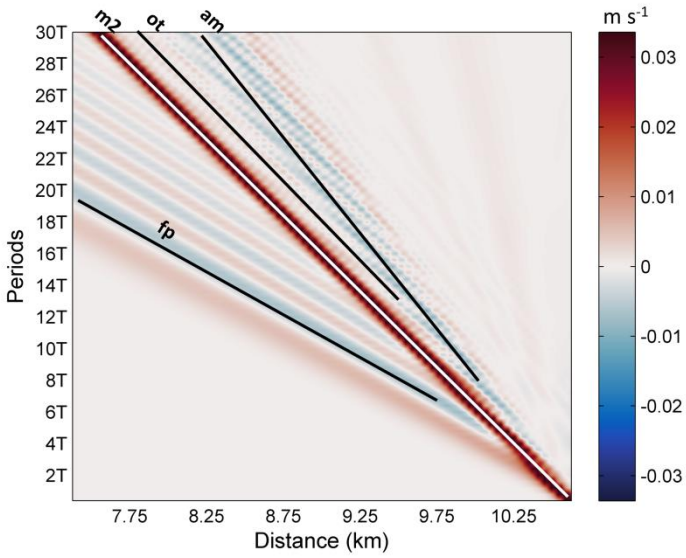

Figure 6. Hovmöller plot of horizontal velocity without background shear current at the surface. The mode-2 ISW, forward-propagating long wave, oscillating tail and amplitude-modulated wave packet are denoted by 'm2', 'fp', 'ot' and 'am', respectively.

3.3 The evolution of mode-2 ISW in case 5

The influence of the offset background shear current on the modulation of mode-2 ISW was investigated, and in offset cases the shear current was set to deviate from the center of pycnocline with varied asymmetry parameters. We take case O9 (Δ = 2) for a detailed examination in the following section.~~In other cases (Δ = 0.5, 1.0, 1.5, 2), the shear current was set to deviate from the pycnocline center to examine the influence of the relative distance on the energy transfer process of mode-2 ISWs. The case 5 (Δ = 2) was examined in the following section.~~ The evolution of the mode-2 ISW in the case ~~5~~ O9 and its corresponding vorticity field are shown in Fig. 7 and Fig. 8, respectively.

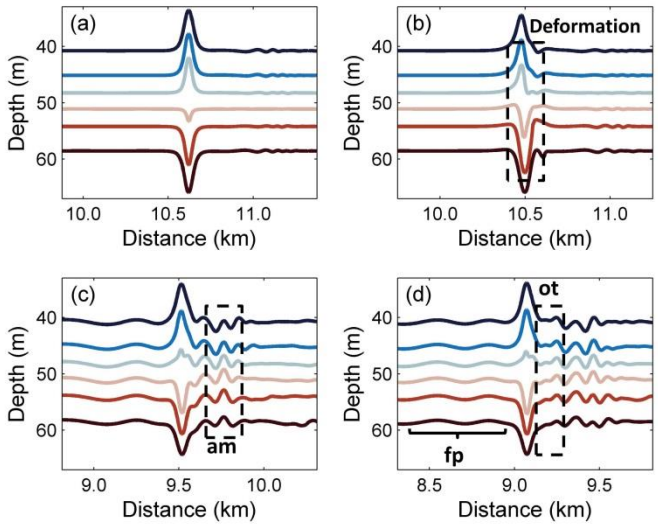

Figure 7: The evolution processes of the mode-2 ISW in the case O9 (Δ = 2.0) for the different times (a) 0T, (b) 1.2T, (c) 10T, (d) 14T, where 'am', 'fp' and 'ot' denote the amplitude-modulated wave packet, forward-propagating long wave and oscillating tail, respectively.

~~**Figure 7:** The evolution processes of the mode-2 ISW in the case 5 (Δ = 2.0) at different times (a) 0T, (b) 1.2T, (c) 10T, (d) 14T.~~

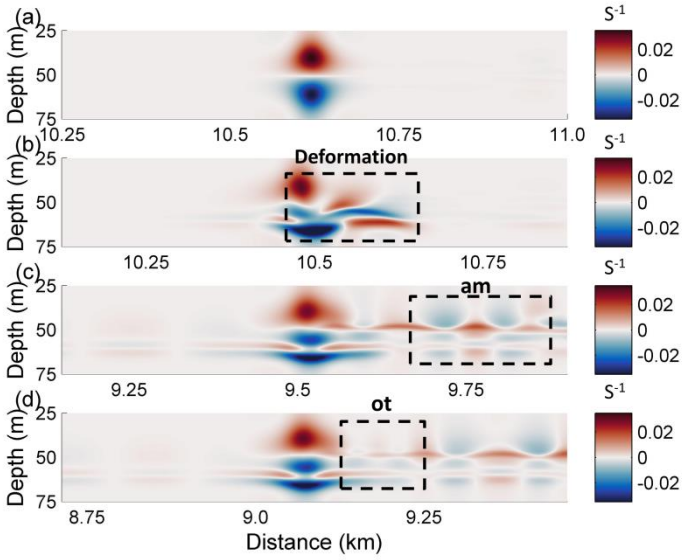

Figure 8. The evolution process of the vorticity field in the case O9 (Δ = 0) for the different times (a) 0T, (b)1.2T, (c) 10T, (d) 14T, where 'am', 'fp' and 'ot' denote the amplitude-modulated wave packet, forward-propagating long wave and oscillating tail, respectively.

~~**Figure 8:** The evolution process of the vorticity field in the case 5 (Δ = 2.0) for different times of (a) 0T, (b)1.2T, (c) 10T, (d) 14T.~~

The deformation of the vortex dipole at 1.2 T after the initialization of background shear current is

illustrated in Fig. 8 (b). The shear vertically distorted the lower section of the vortex and forced some of the vortices from the lower part of the dipole to penetrate the upper part. Redistribution of vorticity occurred both vertically and horizontally. The upper section was bifurcated such that the branch containing most of the vorticity intruded ahead, which related to the generation of a forward-propagating long wave in the same manners at that in the case 1, as shown in Fig. 7 (b). The other branch moved backward to the aft of the ISW, corresponding to the generation of amplitude-modulated wave packet. Given this modulation process, while the lower part of the dipole obviously shrank, the upper parts slowly reunited to restore the vertical balance.

The vorticity distribution was different from that of the case 1 at 10 T~~ after the initialization of background shear current~~ (Fig. 8 (c)). The lower part of the vortex had two obvious cores, which were separated by the shear effect and jointly balanced with the upper section. The amplitude-modulated wave packet and forward-propagating long waves are plotted (Fig. 7 (c)). The amplitude of the wave packet was 1 m, which was smaller than that of the control experiment. However, the amplitude of the forward-propagating long wave was still approximately 0.2 m. In Fig. 7 (d), an oscillating tail with 0.25 m amplitude developed at the rear of the wave. It was sustained by the energy transferred from the ISW, as shown in Fig. 8 (d). ~~The amplitude of the wave packet was 1 m, which was smaller than that of the case 1, suggesting that the energy transfer process was weakened. However, the amplitude of the forward-propagating long wave was still approximately 0.25 m, implying that the forward-propagating long wave may not be affected by the Δ. In Fig. 7 (d), an oscillating tail with 0.25 m amplitude developed at the rear of the wave. It was sustained by the energy transferred from the ISW, as shown in Fig. 8 (d).~~ When the shear current is offset in the upward direction ($\Delta < 0$), the asymmetry of the mode-2 ISW during the modulation became clearer. The amplitude of the oscillating tail and amplitude-modulated wave packet both decreased when the shear current was offset upward, showing a symmetric variation trend with respect to the downward offset condition. For the forward-propagating long wave, its amplitude oscillates by approximately 0.2 m, suggesting the insensitive nature of the long wave to the upward offset shear current. The small amplitude of the oscillating tail and amplitude-modulated wave packet in larger Δ cases indicate that the modulation could be weaker when Δ increased, and the weakening of the oscillating tail makes the amplitude-modulated wave packet more visible.

3.4 The evolution of mode-2 ISW in opposing and polarity-reversal background shear current

The modulation of mode-2 ISW in following (control experiment) and opposing shear current was compared. In case D1, the background shear current oriented against the mode-2 ISW. The general pattern of the forward-propagating long wave, oscillating tail and amplitude-modulated wave packet were similar to those in the control experiment. In this opposing case D1, the amplitude of the forward-propagating long wave and oscillating tail were not significantly affected. For the mode-2 ISW, its amplitude also remains nearly unchanged between the following and opposing cases, while the amplitude-modulated wave packet's amplitude decreased from 1.85 m (following case) to 1.09 m in the opposing case. These results suggest that only the amplitude-modulated wave packet is sensitive to the orientation of the background shear current. The modulation of mode-2 ISW in polarity-reversal shear current was also compared to the control experiment. In case P1, the polarity-reversal background shear current was initialized in the model. The properties of the wave structures in the case P1 and the control experiment were compared and no significant difference were found. Only the polarity of the forward-propagating long wave, oscillating tail and amplitude-modulated wave packet are reversed in case P1. This result indicates that the polarity of those shear-induced wave structures is closely related to the polarity of the background shear current.

3.5 The evolution of mode-2 ISW in background shear current with varied magnitude

The modulations of mode-2 ISWs in variable magnitude of shear currents were characterized. The magnitude of the background shear current was varied from 0.5 U_d to 2.5 U_d from case U1 to case U5 to study its influence on the evolution of the mode-2 ISW. In case U5 (Fig. 9), a relatively larger amplitude forward-propagating long wave was observed at 20 T (Fig. 9 (c)). The mode-2 ISW became inconspicuous at 50 T (Fig. 9 (d)), while an amplitude-modulated wave packet propagated clearly. The increasing magnitude of the background shear current leads to smaller amplitudes of the mode-2 ISW in both upper and lower parts. In the larger magnitude case, the amplitude-modulated wave packet and forward-propagating long wave were significantly strengthened, and their amplitudes reached 3.75 m and 0.38 m (case U5), respectively. In contrast, a larger magnitude didn't make the amplitude of the oscillating tail continue to increase. In the larger magnitude case, the oscillating tail was unable to be clearly observed. Its amplitude becomes smaller (0.25 m) than that of the forward-propagating long wave (0.38 m). In summary, all three shear-induced waves are sensitive to the magnitude of the shear

current.

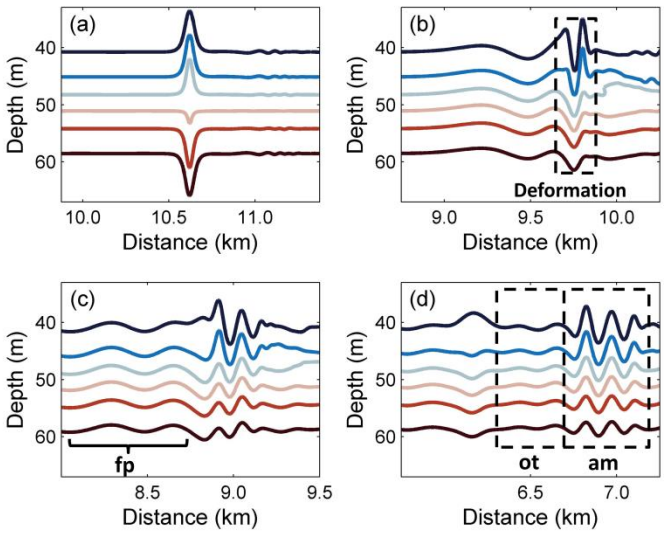

Figure 9. The evolution processes of the mode-2 ISW in the case U5 for the different times (a) 0T, (b) 10T, (c) 20T, (d) 50T, where 'am', 'fp' and 'ot' denote the amplitude-modulated wave packet, forward-propagating long wave and oscillating tail, respectively.

3.6 The evolution of mode-2 ISW in background shear current with varied thickness of shear

The thickness of the shear layer h_s was also varied to investigate its effect on the modulation of mode-2 ISW (cases H1 to H5). In comparison among these cases, the forward-propagating long wave's amplitude decreased with larger h_s, reaching 0.17 m in case H5 with 2.5 h_s. The amplitude-modulated wave packet and oscillating tail both decrease to 1.33 m and 0.42 m in amplitude in larger h_s (case H5), respectively, while the mode-2 ISW's amplitude reaches 7.95 m. This result shows that the background shear current with smaller h_s could only moderately deform the mode-2 ISW. As a result, all three shear-induced wave structures are sensitive to the variation in the thickness of the shear layer.

3. 7 The relationship between the evolution process and variable parameters of background shear current.~~4 The relationship between the energy transfer process and A~~

The amplitudes of the forward-propagating long wave, oscillating tail and amplitude-modulated wave packet in varied background shear currents are summarized to investigate their sensitivity to the varied

background shear currents.~~The amplitude of the different types of waves which were shed from the mode-2 ISWs in five cases are given in Fig. 9 , to reveal the effects of the Δ on the modulation of the mode-2 ISW. Through a comparison of different cases from Δ = 0 (case 1) to Δ = 2 (case 5), the modulation caused by background shear currents have been weakened as the Δ increased, corresponding to the decreased amplitude of the amplitude-modulated wave packet and oscillating tail.~~ The amplitude of the forward-propagating long wave and amplitude-modulated wave packet are positively proportional to the magnitude of the background shear current, but the oscillating tail is insensitive to the higher magnitude of background shear current (Fig. 10 (a)) . The amplitudes of the oscillating tails and amplitude-modulated wave packet are inversely proportional to the thickness of the shear layer, and the forward-propagating long wave decreased slightly in amplitude with increasing h_s (Fig. 10 (b)). To reveal the effects of the Δ on those shear-induced wave structures, a comparison of different cases from Δ = 0 (case O5) to Δ = 2 (case O9) was given. The modulation caused by background shear currents was weakened as the Δ increased, corresponding to the decreased amplitude of the amplitude-modulated wave packet and oscillating tail. The amplitude-modulated wave packet has the highest amplitude among all cases compared to those of the other two wave forms. ~~–~~The amplitude of wave-packet decreased from 1.8 m to 1 m monotonically, and the amplitudes of the oscillating tails decreased from 0.85 m to 0.25 m between the case ~~1~~ O5 (Δ = 0) and the case O7~~3~~ (Δ = 1), but remained stable between the case ~~3~~ O7 (Δ = 1) and case ~~5~~ O9 (Δ = 2), indicating that the amplitude-modulated wave packet were more sensitive to the Δ than the oscillating tail. ~~As the Δ increased, the modulation caused by the background shear current decreased, further causing weakened energy transfer process and shrinking the amplitude.~~ As expected, the ratio between the amplitude of modulated wave packet and oscillating tails increased from 2.1 in the case ~~1~~ O5 to 4 in the case ~~5~~O9, so the amplitude-modulated wave packet became more distinct in case O9~~5~~. ~~The amplitude-modulated wave packet has the highest amplitude among all cases compared to those of the other two wave forms. Thus, amplitude-modulated wave packet could play an important role of energy transfer in the initial stages of the modulation processes.~~ In contrast, the forward-propagating long wave barely affected by Δ and remained constant at approximately 0.2 m in all cases. A similar variation trend could be found in the upward offset cases (Fig .10 (c)). The amplitudes of the oscillating tail and amplitude-modulated wave packet decreased monotonically as the shear current was offset upward. The forward-propagating long wave was barely affected by Δ and remained constant at approximately 0.2 m in all offset cases.

This divergence of sensitivity between the forward-propagating long wave, amplitude-modulated wave packet and oscillating tail could be related to their generation mechanisms, which are discussed in section 5.~~In contrast, the forward-propagating long wave barely affected by Δ and remained constant at approximately 0.25 m in all cases. This divergence of sensitivity between the forward-propagating long wave, amplitude-modulated wave packet and oscillating tail could be related to their generation mechanisms, which needs further study.~~

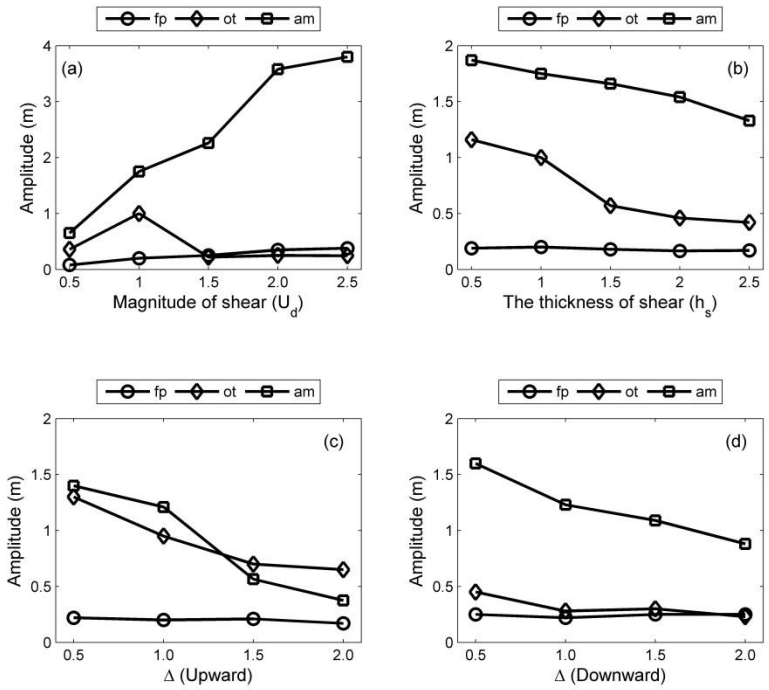

Figure 10. The summarized results of the amplitudes of the forward-propagating long wave (denoted by 'fp'), oscillating tail (denoted by 'ot') and amplitude-modulated wave packet (denoted by 'am') with the presence of (a) varied magnitude of shear currents at 40 T, (b) varied thickness of shear currents at 40 T, (c) upward offset background shear currents at 30 T and (d) downward offset background shear currents at 30 T.

~~**Figure 9:** The amplitude of the different types of waves which were shed from the mode-2 ISWs in five cases are shown; circles represent the forward-propagating long wave, diamonds represent the oscillating tail and squares represent the amplitude-modulated wave packets.~~

4 Energy analyses

4.1 Calculation of energy

The evolution of the mode-2 ISWs in the presence of shear currents was analyzed quantitatively in terms of energy. The available potential energy (APE) and kinetic energy (KE) were calculated based on the method suggested by Lamb (2010):~~of the dissipations were calculated. The equations are~~

$$\mathrm{KE} = \int_{x_l}^{x_r} \int_{-H(x)}^{0} \rho_0 (u^2 + w^2) dx dz, \quad (34)$$

$$\mathrm{APE} = \int_{x_l}^{x_r} \int_{-H(x)}^{0} (\rho - \bar{\rho}) g z dx dz, \quad (45)$$

And the total energy E is written as:

$$\mathrm{E} = \mathrm{KE} + \mathrm{APE}, \quad (56)$$

where $\bar{\rho}$ is the reference density extracted from the initial field, ρ_0 is the averaged density and ρ is the fluid density. x_r and x_l are the boundaries location of the integration region, and the x satisfied $x_l \leq x \leq x_r$. During the calculation of the wave energy, x_r and x_l denote the left and right boundaries, respectively, where the available potential energy flux equals zero (Lamb, 2010). The u and w are the horizontal and vertical velocity induced by the wave, respectively~~, and they were extracted without the background velocity~~. The total energy of the initial mode-2 ISW just before the introduction of the shear calculated by the above expressions was 146.2KJ m^{-1}.

Using the method introduced by Lamb and Nguyen (2009), we set two transects at the front and rear edges of the mode-2 ISW to compute the energy fluxes radiating from the ISW. The total energy flux through a transect is:

$$E_f = KE_f + APE_f + W, \quad (67)$$

where KE_f, APE_f and W are the kinetic, available potential and pressure perturbation energy fluxes, respectively. They are written as:

$$KE_f = \int_{-H(x)}^{0} uKE dz, \quad (78)$$

$$APE_f = \int_{-H(x)}^{0} uAPE dz, \quad (89)$$

$$W = \int_{-H(x)}^{0} up_d dz, \quad (910)$$

where u is the horizontal velocity induced by the mode-2 ISWs, and p_d is the pressure perturbation relative to the reference state (Lamb and Nguyen, 2009).

4.2 The cascading process of energy

To understand better how the mode-2 ISW is modulated with the presence of shear current and to determine the nature of the whole wave system, the EOF (Empirical Orthogonal Function) method was applied to the modal decomposition. It is commonly used for mode decomposition and space-time-distributed datasets examination in oceanography (Venayagamoorthy and Fringer, 2007), especially with strong nonlinearity properties, where the traditional normal mode decomposition is not suitable (Venayagamoorthy and Fringer, 2007).~~The EOF method was applied to the modal decomposition according to Venayagamoorthy and Fringer (2007), since the standard normal modes method is not suitable for the analysis of nonlinear and nonhydrostatic forward propagating long wave, amplitude modulated wave packet and oscillating tail.~~ Because of the shear effect on the mode-2 ISWs, the energy can cascade into all the modes, including mode-1 and higher modes. The vertical and horizontal kinetic energy modal distributions of different wave forms shed from the mode-2 ISW in the case ~~1~~ O5 are shown in Fig. ~~10~~11 and the model structures on waves (Talipova et al., 2011) for different times are given in Fig .12. In the forward-propagating long waves, the kinetic energy was all in the mode-1 form because of its propagation in front of the ISWs, indicating the generation of the forward-propagating long waves corresponds to a cascading process from higher to lower modes. Fig~~ure~~.11~~0~~ shows that the energy was mainly mode-1 in the oscillating tail and the amplitude-modulated wave packet, but weak mode-2 signals were also present~~, which was expected since the oscillating tail and amplitude modulated wave packet follow the mode-2 ISW~~. The presence of mode-2 energy for the oscillating tail and amplitude-modulated wave packet is reasonable because they have shorter wavelengths and slower phase speeds than the mode-2 ISW and propagate following the mode-2 ISW (Akylas and Grimshaw, 1992; Vlasenko et al., 2010). The model structures of forward-propagating long wave for different times show its mode-1 nature was stable during the evolution of mode-2 ISW in the background shear current (Fig. 12 (a) and (b)). In the rear of the mode-2 ISW, the model structures of trailing waves transformed slightly with the time (Fig. 12 (c) – (g)), the wave-induced current are more and more concentrated around the pycnocline far away from the mode-2 ISW.

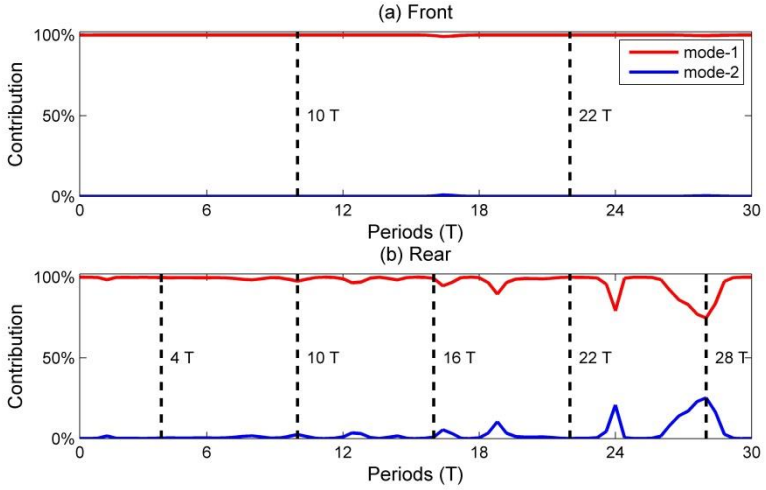

Figure 11. Percent contributions of mode-1 and mode-2 to the total kinetic energy in control experiment (case O5 with Δ = 0) from 0 to 30 T at the (a) front and (b) rear of the mode-2 ISW, the dash lines indicate the cross section where the model structures on waves shown in Figure 12.

~~**Figure 10:** Percent contributions of mode-1 and mode-2 to the total kinetic energy in case 1 (Δ = 0) at 30 T for the (a) forward-propagating long wave, (b) oscillating tail and (c) amplitude-modulated wave packet.~~

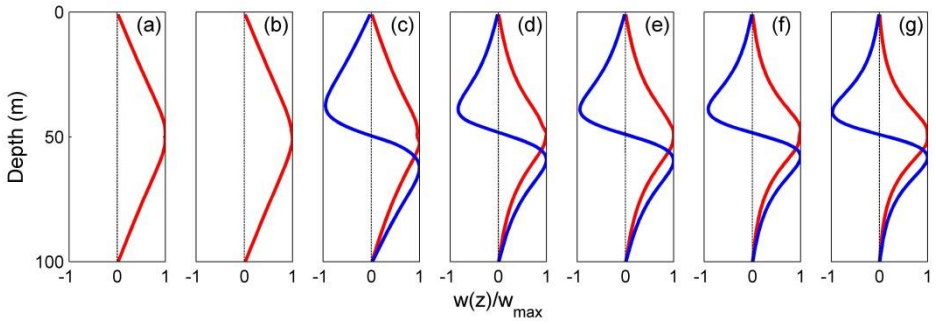

Figure 12. The model structures on mode-1 (red solid line) and mode-2 (blue solid line) waves in front of the mode-2 ISW at (a) 10 T, (b) 22 T and in rear of the mode-2 ISW at (c) 4 T, (d) 10 T, (e) 16 T, (f) 22 T and (g) 28 T for control experiment (case O5).

4.3 Energy loss of mode-2 ISW

The energy loss of mode-2 ISW in control experiment was investigated in detail to demonstrate the corresponding energy changing process during the modulation and compared with the observations of Shroyer et al. (2010).In ~~the~~ this case 1, ~36% of the total energy of the mode-2 ISW was lost by 30 T, corresponding to a propagation of 1.86 km, part of that energy was transferred to ~~other~~ shear-induced

wave forms. During the first 30 T, The average energy loss rate was 9 W/m. Modulated by background shear current, the mode-2 ISW exhibits a highly dissipated nature, and the high energy loss rate is comparable to that of the longer mode-1 ISW (Lamb and Farmer, 2011; Shroyer et al., 2010). This quantitative result was consistent with the observation data (Shroyer et al., 2010). ~~, such that all of the energy of the mode-2 ISW would be drained in 4.5 h, or by approximately 82 T, as we defined above, with a propagation distance of ~5 km. Modulated by the background shear current, the mode-2 ISW exhibits a "short-lived" nature and high energy loss rate, which is comparable to that of the longer mode-1 ISW (Lamb and Farmer, 2011; Shroyer et al., 2010).~~

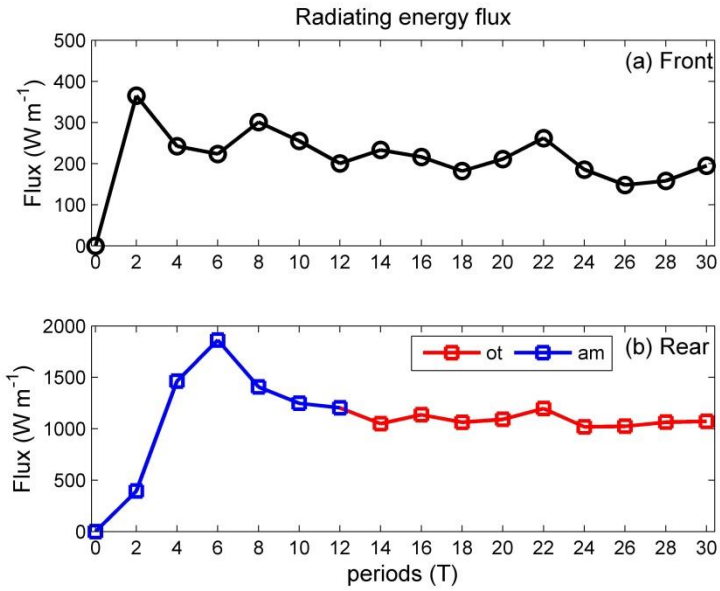

Figure 13. Vertical integrals of the radiating energy flux in the (a) front and (b) rear transects of the mode-2 ISW in control experiment (case O5 with Δ = 0) at different times, where "ot" denotes the oscillating tail and "am" denotes the amplitude-modulated wave packet.

~~**Figure 11:** Vertical integrals of the radiating energy flux in the (a) front and (b) rear transects of the mode-2 ISW in case 1 (Δ = 0) at different times.~~

We further calculated the radiating energy flux (Fig. 13) to investigate the detailed energy transport. The pressure perturbation generally make the largest instantaneous contributions to the total energy flux (Lamb and Nguyen, 2009; Venayagamoorthy and Fringer, 2007). For an ISW, the pressure perturbation term could be dominant (Lamb 2007). Since we focused on the energy loss of the mode-2 ISW, only a total energy flux was analyzed in the following paragraph. The radiating energy flux in the front transect slowly decreased, indicating the forward-propagating long wave drains the energy of the mode-2 ISW at a decreasing rate in the presence of a background shear current.~~For the case 1, we~~

~~calculated the radiating energy flux (Fig. 11) to investigate the detailed energy transport. The radiating energy flux in the front transect was nearly constant at approximately 0.2 KW m^{-1}, indicating the forward propagating long wave drains the energy of the mode-2 ISW at a constant rate in the presence of a background shear current.~~ In the rear transect, the radiating energy flux decreased from 1.8 KW m^{-1} to 1.2 KW m^{-1} before stabilizing at approximately 1.0 KW m^{-1} above 12 T. The energy flux at the crest of the amplitude-modulated wave packet and the oscillating tail ranged from 1.0 KW m^{-1} to 2.0 KW m^{-1} (Blue solid line in Fig. 12) and 1.0 KW m^{-1} to 1.1 KW m^{-1}, respectively.~~The energy flux at the crest of the amplitude-modulated wave packet and the oscillating tail ranged from 1.0 KW m^{-1} to 2.5 KW m^{-1} and 0.3 KW m^{-1} to 1.1 KW m^{-1}, respectively.~~ Combining with the evolution process, the high radiating flux before 12 T indicates the generation process of the amplitude-modulated wave packet and that the relative low radiating energy flux above 12 T is caused by the generation of an oscillating tail.

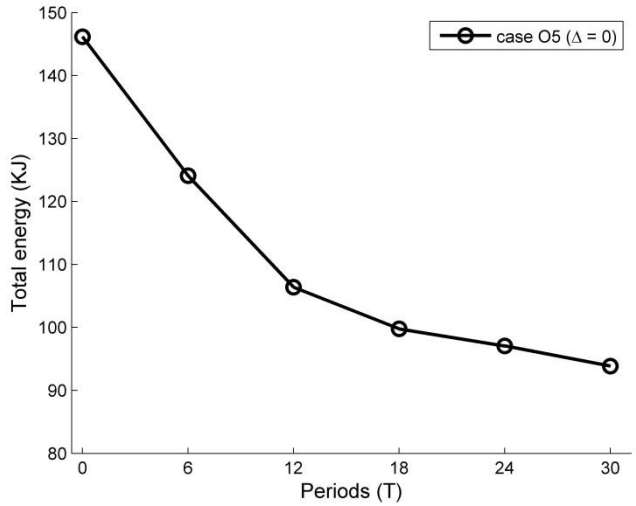

Figure 14. The total energy of the ISW at the different times in case O5

~~**Figure 12:** The total energy of the ISW in the different times and cases; circles represent the case 1 (Δ = 0), diamonds represent the case 2 (Δ = 0.5), squares represent the case 3 (Δ = 1.0), triangles represent the case 4 (Δ = 1.5) and crosses represent the case 5 (Δ = 2.0).~~

The total energy of the mode-2 ISWs ~~in the~~at different ~~cases and~~ times in control experiment are shown in Fig. ~~12~~14~~, and the averaged energy loss rates at each period are given in Table 2~~. From 0 to 6 T, the averaged energy loss rate~~s decreased significantly, from~~ was18.4 W m^{-1} ~~(case 1) to 0.4 W m^{-1} (case 5)~~. This period corresponded to the generation of the amplitude-modulated wave packet and forward-propagating waves, during which a deformation was caused by the shear to the aft of the ISW. The averaged energy loss rates from 6 to 12 T decreased~~, decreasing as the Δ increased~~. This stage

contained the exit of the amplitude-modulated wave packet, which occurred at approximately 10 T (Fig. ~~5~~ 4 and Fig. 7), and the generation of the oscillating tail. In ~~the~~ this case ~~1~~, ~34% of the total energy loss (52.34KJ m^{-1}) lost at an average rate of 14.8 W m^{-1} from 6 to 12 T, and some of the energy transferred to the amplitude-modulated wave packet. Combining the results of the energy flux in front and rear of the mode-2 ISW (Fig. 13), thus, in the early stage of modulation, the amplitude-modulated wave packet could make larger contribution to the energy transfer process. ~~High energy loss rate shown in Table 2 could be explained by this transfer process. Thus, in the early stage of modulation, the amplitude-modulated wave packet was suggested occupying an important role of energy transfer process.~~ After the amplitude-modulated wave packet shed from the mode-2 ISWs, sharply decreased loss rates could be seen in 12 – 18 T, during which the energy loss was caused by the forward-propagating long waves and the oscillating tail. The shear currents continuously sustained the development of the oscillating tail and the forward-propagating long waves. Thus, these two forms could slowly drain the energy of the ISW, with an average rate of 3.5 W m^{-1} ~~in the case 1~~. In the following periods, with the forward-propagating long waves and oscillating tails, the ISWs decayed with a relatively low rate.~~In the following periods, with the nearly constant forward-propagating long waves and oscillating tails, the ISWs decayed with a relatively low rate.~~ This was reinforced by a similar result given by Olsthroon et al. (2013).

4.3 The relationship between the energy loss of mode-2 ISW and variable parameters of background shear current

We summarized the effect of variable parameters of shear current on the energy loss of mode-2 ISW during the modulation (Fig. 15). The polarity and the direction of the background shear current have minor effect on the energy loss of mode-2 ISWs. The energy loss of the mode-2 ISW was positively proportional to the magnitude of shear current, but reverse proportional to the thickness of shear layer (Fig. 15 (a) and (b)). For case U5, 78.04 KJ m^{-1} energy loss in 30 T, ~53% of total energy of mode-2 ISW and the averaged energy loss rate was 13 Wm^{-1}, indicating the magnitude of shear could significantly increase the energy loss of mode-2 ISW. in contrast, for case H5, 42.05 KJ m^{-1} energy loss in 30 T, ~29% of total energy of mode-2 ISW and the averaged energy loss rate was 7W m^{-1}, showing that a larger thickness of shear has opposite effect on the energy loss of mode-2 ISW. In the offset background shear currents, the energy loss of mode-2 ISW monotonically decreased with an increasing

Δ, showing a symmetric trend in both upward and downward offset cases (Fig. 15 (c) and (d)). Therefore, the energy losses of mode-2 ISWs are sensitive to the magnitude, thickness and offset extent, but insensitive to the polarity and direction of background shear current.

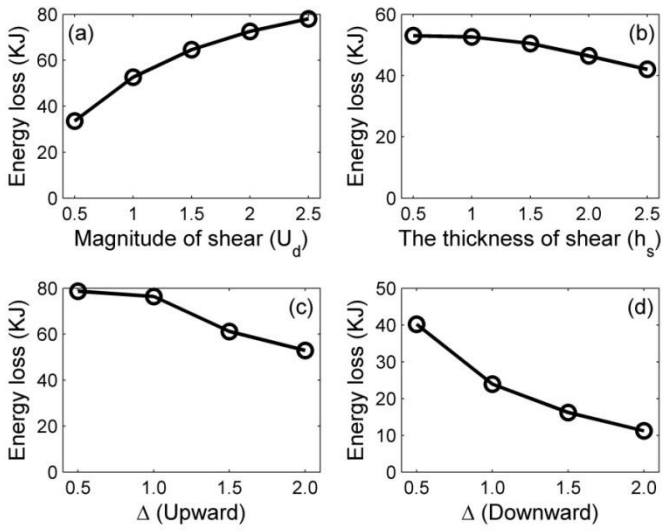

Figure 15. The summarized results of the energy loss of the mode-2 ISW at 30 T with the presence of (a) varied magnitude of shear currents, (b) varied thickness of shear currents, (c) upward offset background shear currents and (d) downward offset background shear currents.

~~**Table 2:** The energy loss rates (W m^{-1}) of the ISWs in different cases at different times.~~

	~~0 – 6 T~~	~~6 T – 12 T~~	~~12 T – 18 T~~	~~18 T – 24 T~~	~~24 T – 30 T~~
~~**Case 1 (Δ = 0)**~~	~~18.4~~	~~14.8~~	~~5.6~~	~~2.3~~	~~2.7~~
~~**Case 2 (Δ = 0.5)**~~	~~12.5~~	~~13.5~~	~~4.2~~	~~2.3~~	~~1.1~~
~~**Case 3 (Δ = 1.0)**~~	~~5.1~~	~~10.3~~	~~3.5~~	~~0.8~~	~~0.37~~
~~**Case 4 (Δ = 1.5)**~~	~~1.7~~	~~8.2~~	~~3.4~~	~~0.2~~	~~0.15~~
~~**Case 5 (Δ = 2.0)**~~	~~0.4~~	~~5.9~~	~~3.0~~	~~0.05~~	~~0.06~~

~~The energy loss rate of the case 1 was obviously higher than that of other cases, since the amplitude of those mode-1 waves was largest among the cases. The energy loss decreased as the Δ increased, which corresponded to monotonic decrease of the amplitudes of different mode-1 wave forms. After 12 T, the~~

~~energy loss rates in the different cases became smaller, since the oscillating tail and forward propagating long waves with a relatively low energy transfer rate lead to the energy loss of mode-2 ISW. Hence, the strength of energy loss of mode-2 ISW can be predicted by the Δ at the early stage of modulation.~~

5 Discussions

We compared our results of the control experiment (case O5) with the observation of Shroyer et al. (2010) for validation. The wavelengths and amplitudes of the initialized mode-2 ISWs were selected to be comparable to the observation of Shroyer et al. (2010) on the New Jersey Shelf.~~In the simulations of the present study, the wavelengths and amplitudes of mode-2 ISWs were selected to be comparable to the observations. Among those cases, the case 2 correspond to the observation by Shroyer et al. (2010) since the center of shear current was displaced by a similar distance from the pycnocline center.~~ A depression wave at the rear of the ISW in the first transect of wave *Jasmine* was similar to the wave form around 10 T in the numerical simulation (Fig. 3 (a) in Shroyer et al., 2010). Thus the first, second and third transects of wave Jasmine corresponded to 10 T, 23 T and 38 T in the case ~~2~~O5, respectively. The energy loss rates in 10 T and 23 T were 14.8 W m^{-1} and 2.3 W m^{-1}, the averaged energy loss rate between 10 T and 38 T was 4.1 W m^{-1}, they were in same scale with the corresponding observations. Between 10 T and 38 T, ~16% of mode-2 ISW total energy lost，it was a little smaller than the typical observation results.~~The energy loss rates in 10 T and 23 T were 13.5 W m^{-1} and 2.3 W m^{-1}, the averaged energy loss rate between 10 T and 38 T was 5.1 W m^{-1}, they were in same scale with the corresponding observations. Between 10 T and 38 T, ~20% of mode-2 ISW total energy lost，it was a little smaller than the typical observation results.~~ Relatively high energy loss rate and a large amplitude oscillating tail in the third transect of the field observations could be probably attributed to the effect of a shoaling pycnocline (Shroyer et al., 2010) and ~~thus~~ since the enhancement of the asymmetries in stratification~~, which~~ could increase the energy loss of the wave during the propagation of mode-2 ISWs (Carr et al., 2015; Olsthoorn et al., 2013).

We also compared our results with Stastna et al. (2015), who investigated the mode-2 ISW interaction with mode-1 ISW at the same scale. The authors concluded that the shear current is vital, while the deformation of the pycnocline only slightly altered the structure of the mode-2 ISW. For our results, we

focused on the effect of shear currents induced by baroclinic eddies, baroclinic tides or wind. We found a deformation of mode-2 ISW and it illustrated asymmetry during the modulation in the presence of background shear current, it is coincident with the conclusion given by Stastna et al. (2015).

Then, we further discussed the characteristics of shear-induced waves. In our simulations, the modulation of mode-2 ISW in the presence of shear currents excites the amplitude-modulated wave packet with characteristics of breather-like internal wave (Terletska et al., 2016). Internal breather waves are periodically pulsating, isolated wave forms, they are also a type of steady state wave solution of the extended Korteweg-de Vries equation (Lamb et al., 2007), and has been found to exist in the real ocean (Vlasenko and Stashchuk, 2015). We introduced the definition of breather by Clarke et al. (2000) to clarify the characteristics of amplitude-modulated wave packet. The envelop lines of the amplitude-modulated wave packet in case O5 are shown in Fig. 16. Inside the envelop lines, the oscillatory pulses freely oscillate, satisfying the breather definition. Additionally, the energy inside the envelope was calculated and remains nearly constant from 12 to 28 T. Similar to the case O5, the characteristics and energy loss of the amplitude-modulated wave packet for the case O9 were also similar with the breather definition. Similar results were revealed by Terletska et al. (2016), the interaction of mode-2 internal waves with a step-like topography could induce the generation of BLIWs (breather-like internal waves), providing a possibility of the breather generation in a thin intermediate layer with a range of intermediate wavelength.

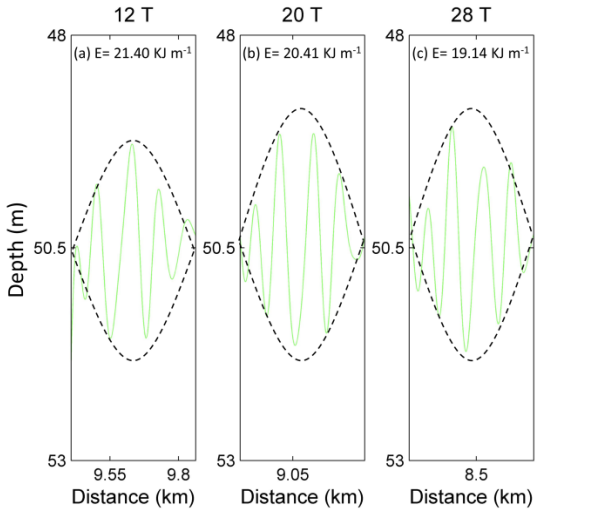

Figure 16. The envelopes of the amplitude-modulated wave packet in the case O5 ($\Delta = 0$) at (a) 12 T, (b) 20 T and (c) 28 T, where the mean density isopycnal of upper and lower layer (green line) are plotted..

An oscillating tail induced by shear was also observed in similar studies (Carr et al., 2011, Stamp and Jacka, 1995). The generation of this feature could be related to the shear, and the tail was sustained by continuous energy input. The presence of the background shear current modulated the mode-2 ISW and induced the continuously energy transfer process from the main wave to the oscillating tail, supporting its existence. Forward-propagating long waves were also observed by Yuan et al. (2018), who found that some small but significant long wavelength mode-1 waves appeared ahead of mode-2 ISWs. The forward-propagating long wave was generated by the collapse of mixing induced by shear instability, and it could drain the energy of mode-2 ISWs at a decreasing rate, leading to an inevitable energy loss of those mode-2 ISWs in the presence of background shear. The results in section 3.8 show that the amplitude of the forward-propagating long wave is proportional to the magnitude of the shear current, indicating that the forward-propagating long wave was affected by the strength of shear. Δ denotes the offset extent of the background shear current, and the strength of the shear remains unchanged when Δ varied. Therefore, the forward-propagating long wave was insensitive to variation in Δ.

The mechanism of adjustment during the modulation has been reviewed. The superposition of an initially stable shear current and the mode-2 ISW induced low Ri region with a minimum value of less than 0.01, indicating a possible development of shear instability (Barad and Fringer, 2010). ~~indicating the possible development of shear instability~~. The ISW tends to adjust gradually and adapt to the new background conditions. The vorticity and Ri of adjustment process for the mode-2 ISW in the case ~~1~~ O5 is shown in Fig. ~~13~~17. The Ri values are larger than 0.25 before 0.8 T. After 0.8 T, due to the shear currents and weakened stratification, the lowest Ri values decrease below 0.01 and are accompanied by increased vorticity around the low Ri region, indicating the generation of shear instability (Pawlak and Armi, 1998). The overturning in isopycnal could be also observed in corresponding low Ri region (Fig. 18). Then, the Ri values increased larger than 0.25, and the stratification is restored above 6.8 T. For the case ~~5~~ O9 (Fig. ~~14~~19), before 0.8 T, the Ri values are also larger than 0.25. They decrease below 0.01 near the depths of the shear current after 0.8 T, which is accompanied by the increased vorticity and weakened stratification, indicating the occurrence of the shear instability. The stratification is restored and the Ri values increased larger than 0.25 after 2 T. Compared to the case ~~1~~O5, the region with low Ri and increased vorticity was smaller in the case ~~5~~O9, making the instability process was less apparent, and the shear instability for the case ~~1~~ O5 occurs at the same time but lasts longer than that for the case

~~5~~O9.

Those comparison illustrated the adjustment of mode-2 ISWs modulated by shear current are more energetic in overlap cases compared to offset cases.

~~Those comparison illustrated the adjustment of mode-2 ISWs modulated by the shear current are more energetic with small Δ, it is consistent with the results that the case 1 has the largest energy loss rate among all cases.~~

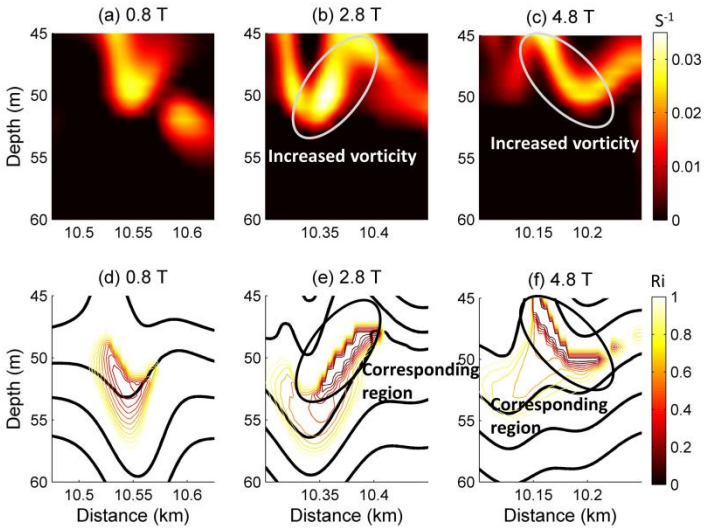

Figure 17. The vorticity spatial distributions for the case O5 (Δ = 0) at (a) 0.8 T, (b) 2.8 T, (c) and 4.8 T, and the corresponding Ri values (ranges from 0 to 1)at (d) 0.8 T, (e) 2.8 T, and (f) 4.8 T.

~~**Figure 13:** The vorticity spatial distributions for the case 1 (Δ = 0) at (a) 0.8 T, (b) 2.8 T, (c) and 4.8 T, and the corresponding Ri values at (d) 0.8 T, (e) 2.8 T, and (f) 4.8 T.~~

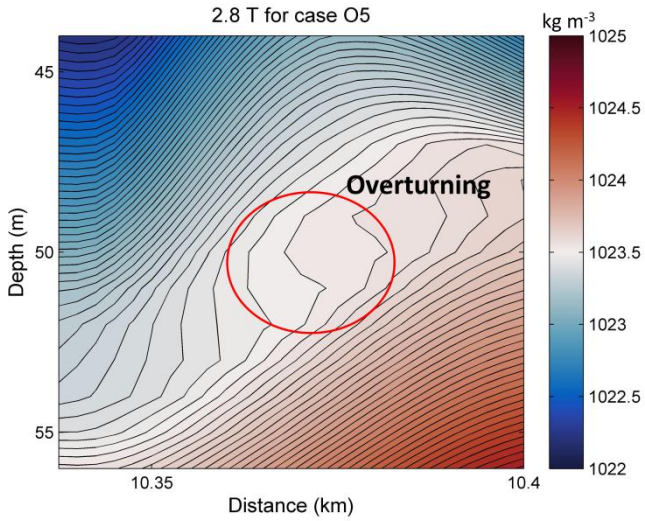

Figure 18. The density contour plot at 2.8 T for the case O5.

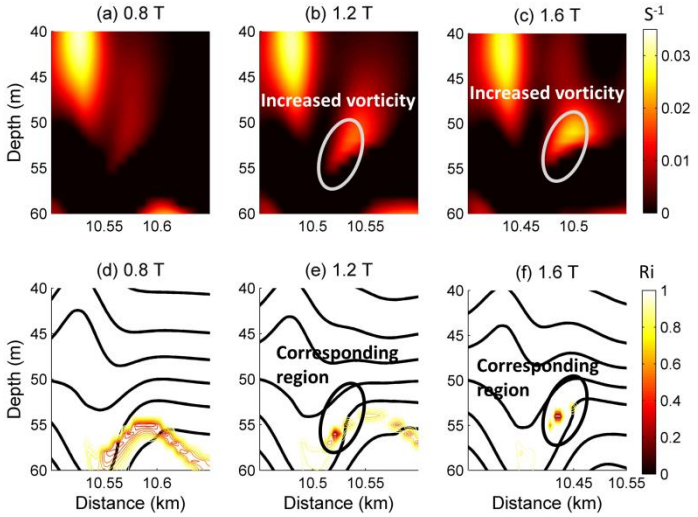

Figure 19. The vorticity spatial distributions for the case O9 (Δ = 2) at 0.8 T (a), 1.2 T (b), and 1.6 T (c), and the corresponding Ri values (ranges from 0 to 1) at 0.8 T (d), 1.2 T (e), and 1.6 T (f).

As for the long-term behavior, the mode-2 ISW could adjust itself to adapt to new background conditions and experience a dramatic transformation with disintegration into a wave train (Grimshaw et al., 2010, Yuan et al., 2018). In our simulation, the mode-2 ISW was observed to adjust itself to the new background condition with a shear current. The high energy loss rate is in agreement with the observation by Shroyer et al. (2010). However, the mode-2 ISW might not be able to survive for long time in situ because the background conditions in real ocean could be more complex and vary with time, leading to a background condition where a stable solution of mode-2 ISW does not exist.

~~**Figure 14:** The vorticity spatial distributions for the case 5 (Δ = 2) at 0.8 T (a), 1.2 T (b), and 1.6 T (c), and the corresponding Ri values at 0.8 T (d), 1.2 T (e), and 1.6 T (f).~~

~~In our simulations, the modulation of mode-2 ISW in the presence of shear currents excites the amplitude-modulated wave packet, whose characteristics are similar to a breather-like internal wave (Terletska et al., 2016). Internal breather waves are periodically pulsating, isolated wave forms, they are also a type of steady-state wave solution of the extended Korteweg-de Vries equation (Lamb et al., 2007), and has been found to exist in the real ocean (Vlasenko and Stashchuk, 2015). We introduced the definition of breather by Clarke et al. (2000) to clarify the characteristics of amplitude-modulated wave packet. The envelop lines of the amplitude-modulated wave packet in case 1 are shown in Fig. 15. Inside the envelop lines, the oscillatory pulses freely oscillate, satisfying the breather definition. Additionally, the energy inside the envelope was calculated and remains nearly constant from 12 to 28~~

~~T. Similar to the case 1, the characteristics and energy loss of the amplitude-modulated wave packet for the case 5 were also similar with the breather definition. Noted that the breather solution exist only if the cubic nonlinearity coefficients in Gardner equation is positive (Lamb et al., 2007), but the configuration of the stratification in our simulation results a negative cubic nonlinearity coefficient in Gardner equation (Grimshaw et al., 2010; Talipova et al., 2011) and it means the breather is not allowed in this stratification. Similar results were revealed by Terletska et al. (2016), the interaction of mode-2 internal waves with a step-like topography could induce the generation of BLIWs (breather-like internal waves), providing a possibility of the breather generation in a thin intermediate layer with a range of intermediate wavelength.~~

~~**Figure 15:** The envelopes of the amplitude-modulated wave packet in the case 1 ($\Delta = 0$) at (a) 12 T, (b) 20 T and (c) 28 T.~~

~~The oscillating tail was frequently observed in similar studies (Carr et al., 2015; Olsthoorn et al., 2013; Stastna et al., 2015). Its generation was related to the shear, and the tail was sustained by continuous energy input. The presence of the background shear current modulated the mode-2 ISW and induced the continuously energy transfer process from the main wave to the oscillating tail, supporting its existence. Forward-propagating long waves were also observed in Terletska et al. (2016). A forward-propagating long wave with nearly constant amplitude could drain the energy of mode-2 ISWs at a steady rate, and then leads to an inevitable energy loss of those mode-2 ISWs in the presence of background shear.~~

~~The numerical simulation results shown above indicate the amplitude-modulated wave packet, oscillating tails and forward-propagating long waves were generated during the adjustment of the mode-2 ISWs in the presence of the shear currents. Those wave forms are common in the adjustment of mode-2 ISWs (Carr et al., 2015; Olsthoorn et al., 2013; Terletska et al., 2016), but the generation mechanism of amplitude-modulated wave packet requires further examination.~~

6 Conclusions

We have presented the evolution process of mode-2 ISWs modulated by varied~~the~~ background shear current with the MITgcm in this study. It was illustrated that the adjustment of the mode-2 ISWs in the

presence of background shear current occurs through the generation of forward-propagating long waves, amplitude-modulated wave packet, and an oscillating tail.~~We illustrated the adjustment of the mode-2 ISWs in the presence of background shear current occurs through the generation of forward-propagating long waves, amplitude-modulated wave packet, and an oscillating tail.~~

For comparison with the observation, a control experiment was conducted (case O5).~~Five different cases with different Δ were introduced to assess the sensitivity of the energy transfer process to the Δ. From the comparison between different cases, we have found the amplitude-modulated wave packets were the most sensitive to the Δ, followed by the oscillating tails, while the forward-propagating long waves were robust to different Δ. The amplitude-modulated wave packet was suggested playing an important role in energy transfer process during the early stage of modulation. The energy analysis of case 1 demonstrated in the first 30 periods,~~ ~36% of the total energy of the mode-2 ISW was lost at an average rate of 9 W m^{-1}, and this rate was in agreement with the observation of Shroyer et al. (2010). The mode-2 ISWs are highly dissipated in the presence of shear currents,~~which would deplete the energy of mode-2 ISW in ~4.5 h, corresponding to a propagation distance of ~5 km. Thus, we concluded the mode-2 ISWs are ephemeral in the presence of shear currents,~~ In addition, 5 sets of experiments were introduced to assess the sensitivity of the evolution process to different properties of the background shear currents in order to get general conclusion. We found that the polarity and direction of the background shear current have minor effect on the evolution of the mode-2 ISW. The amplitudes of the forward-propagating long wave and amplitude-modulated wave packet as well as the decaying of mode-2 ISWs' energy are positively proportional to the magnitude of shear but negatively proportional to the thickness of the shear layer. We also found that the oscillating tail and amplitude-modulated wave packet show symmetric variation trend in both offset upward and downward conditions, while the forward-propagating long wave was insensitive to the background shear current, and the shear layers centered at the mid-depth of pycnocline had much more pronounced energy loss of the mode-2 ISW compared to those cases where the shear layer centered away from the mid-depth of the pycnocline.~~and it was consistent with the hypothesis given by Shroyer et al. (2010). The ISW energy loss rates were found to decrease monotonically as the Δ increased which mean those wave forms shed from the mode-2 ISW were more energetic in small Δ cases. In future work, a detailed investigation of generation mechanisms of different wave forms shed from the mode-2 ISW are needed to explain the divergence in their sensitivity to the Δ.~~

In future work, a possible avenue is the evolution of mode-2 ISW in time-varied background shear current, and the wave-mean flow interaction in this complicated flow fields, revealing the energy exchange process between waves and mean-flow. The other possible direction is the investigation of combination effect which is more close to field observations on the evolution of the mode-2 ISW, including the effect of background shear current, varying topography and shoaling pycnocline.

Acknowledgments

Funding for this study was provided by National Key Research and Development Program of China (No. 2017YFA0604102), the Scientific and Technological Innovation Project Financially Supported by QNLM (No. 2016ASKJ12), National Key Research and Development Program of China (No. 2016YFC1401404), the National Natural Science Foundation of China (41528601, 41676006, 41421005), Youth Innovation Promotion Association CAS, CAS Interdisciplinary Innovation Team, Key Research Program of Frontier Science, CAS, and the Strategic Pioneering Research Program of CAS, (XDA11020104, XDA11020101). This study was supported by the High Performance Computing Center at the IOCAS. Constructive and helpful comments from the editor, Prof. Tatiana Talipova, and two anonymous reviews are gratefully acknowledged. The MITgcm program can be downloaded from the websites at http://mitgcm.org. The EOF codes can be downloaded from http://cn.mathworks.com/matlabcentral/fileexchange. The simulation data deposit for this paper needs high-capacity disk and is available on the request to Dr. Zhenhua Xu by email.

References

Akylas, T. R., & Grimshaw, R. H. J. Solitary internal waves with oscillatory tails. J.Fluid Mech, 242, 279-298, 1992.

Barad M F, Fringer O B. Simulations of shear instabilities in interfacial gravity waves[J]. Journal of Fluid Mechanics, 644: 61-95, 2010.

Brandt, A., & Shipley, K. R. Laboratory experiments on mass transport by large amplitude mode-2 internal solitary waves. Phys.Fluids, 26(4), 016602-82, 2014.

Carpenter J R, Balmforth N J, Lawrence G A. Identifying unstable modes in stratified shear layers[J].

Physics of Fluids, 22(5): 054104, 2010.

Carr, M., Davies, P. A., &Hoebers, R. P. Experiments on the structure and stability of mode-2 internal solitary-like waves propagating on an offset pycnocline. Phys.Fluids, 27(4), 046602, 2015.

Carr M, King S E, Dritschel D G. Numerical simulation of shear-induced instabilities in internal solitary waves[J]. Journal of Fluid Mechanics, 683: 263-288, 2011.

Chen, G. Y., Liu, C. T., Wang, Y. H., & Hsu, M. K. Interaction and generation of long‐crested internal solitary waves in the South China Sea. J.Geophys.Res., 116(C6), 1-7, doi:10.1029/2010JC006392, 2011.

Clarke, S., Grimshaw, R., Miller, P., Pelinovsky, E., & Talipova, T. On the generation of solitons and breathers in the modified Korteweg–de Vries equation. *Chaos:* An Interdisciplinary Journal of Nonlinear Science, 10(2), 383-392, 2000.

Deepwell, D., &Stastna, M. Mass transport by mode-2 internal solitary-like waves. Phys.Fluids,28(5), 395-425, 2016.

Duda T F, Lynch J F, Irish J D, et al. Internal tide and nonlinear internal wave behavior at the continental slope in the northern South China Sea[J]. IEEE Journal of Oceanic Engineering, 29(4): 1105-1130, 2004.

Farmer, D., Li, Q., & Park, J. H. Internal wave observations in the South China Sea: The role of rotation and non‐linearity. Atmosphere-Ocean, 47(4), 267-280, 2009.

Grimshaw R, Pelinovsky E, Talipova T. Modelling internal solitary waves in the coastal ocean[J]. Surveys in Geophysics, 28(4): 273-298, 2007.

Grimshaw, R., Pelinovsky, E., Talipova, T., & Kurkina, O. Internal solitary waves: propagation, deformation and disintegration. Nonlinear Processes in Geophys., 17(6), 633, 2010.

Helfrich, K. R., & Melville, W. K. On long nonlinear internal waves over slope-shelf topography. J.Fluid Mech.,167(167), 285-308, 1986.

Helfrich, K. R., & Melville, W. K. Long nonlinear internal waves. Annu. Rev. Fluid Mech., 38, 395-425, 2006.

Hüttemann, H., &Hutter, K. Baroclinic solitary water waves in a two-layer fluid system with diffusive interface. Exp.Fluids,30(3), 317-326, 2001.

Jackson C R, da Silva J C B, Jeans G, et al. Nonlinear internal waves in synthetic aperture radar imagery[J]. Oceanography, 26(2): 68-79, 2013.

Klymak, J. M., & Moum, J. N. Internal solitary waves of elevation advancing on a shoaling shelf. Geophys.Res.Lett., 30(20), 2003.

Lamb K G. Energetics of internal solitary waves in a background sheared current[J]. Nonlinear Processes in Geophysics, 17(5): 553, 2010.

Lamb, K. G. Internal wave breaking and dissipation mechanisms on the continental slope/shelf. Ann. Rev. Fluid Mech., 46, 231-254, 2014.

Lamb, K. G., & Farmer, D. (2011). Instabilities in an internal solitary-like wave on the oregon shelf. J.Phys.Oceanogr., 41(1), 67-87, 2011.

Lamb, K. G., & Nguyen, V. T. Calculating energy flux in internal solitary waves with an application to reflectance. J.Phys.Oceanogr., 39(3), 559-580, 2009.

Lamb, K. G., Polukhina, O. E., Talipova, T., Pelinovsky, E., Xiao, W., & Kurkin, A. Breather generation in fully nonlinear models of a stratified fluid. Phys.Rev.E, 75(4), 2007.

Legg, S., & Adcroft, A. Internal wave breaking at concave and convex continental slopes. J.Phys.Oceanogr, 33(11), 2224-2246, 2003.

Legg, S., & Huijts, K. M. Preliminary simulations of internal waves and mixing generated by finite amplitude tidal flow over isolated topography. Deep Sea Research Part II: Topical Studies in Oceanography, 53(1), 140-156, 2006.

Legg, S., & Klymak, J. (2008). Internal hydraulic jumps and overturning generated by tidal flow over a tall steep ridge. J.Phys.Oceanogr, 38(9), 1949-1964, 2008.

Liu, A. K., Chang, Y. S., Hsu, M. K., & Liang, N. K. Evolution of nonlinear internal waves in the East and South China Seas. J.Geophys.Res, 103(C4), 7995-8008, 1998.

Liu, A. K., Ramp, S. R., Zhao, Y., & Tang, T. Y. A case study of internal solitary wave propagation during ASIAEX 2001. IEEE J.Oceanic Eng., 29(4), 1144-1156, 2004.

Liu, A. K., Su, F. C., Hsu, M. K., Kuo, N. J., & Ho, C. R. Generation and evolution of mode-two internal waves in the South China Sea. Cont.Shelf Res., 59, 18-27, 2013.

Marshall, J., Hill, C., Perelman, L. T., &Adcroft, A. Hydrostatic, quasi-hydrostatic, and nonhydrostatic ocean modeling. J.Geophys.Res., 5733-5752, 1997.

Moum, J. N., Klymak, J. M., Nash, J. D., Perlin, A., & Smyth, W. D.Energy transport by nonlinear internal waves. J.Phys.Oceanogr.,37(7), 1968-1988, 2006.

Olsthoorn, J., Baglaenko, A., &Stastna, M. Analysis of asymmetries in propagating mode-2 waves.

Nonlinear Processes in Geophys.,20(1), 59-69, 2013.

Pawlak, G., & Armi, L. Vortex dynamics in a spatially accelerating shear layer. J.Fluid Mech., 376, 1-35, 1998.

Ramp, S. R., Yang, Y. J., Reeder, D. B., & Bahr, F. L. Observations of a mode-2 nonlinear internal wave on the northern heng-chun ridge south of taiwan. J.*Geophys.Res.,117(C*3), 3043, 2012.

Salloum, M., Knio, O. M., & Brandt, A. Numerical simulation of mass transport in internal solitary waves.Phys.Fluids,24(24), 21-110, 2012.

Shroyer, E. L., Moum, J. N., & Nash, J. D. Mode 2 waves on the continental shelf: ephemeral components of the nonlinear internal wavefield. J.Geophys. Res.,115(C7), 419-428, 2010.

Stamp A P, Jacka M. Deep-water internal solitaty waves[J]. Journal of Fluid Mechanics, 305: 347-371, 1995.

Stastna M, Lamb K G. Large fully nonlinear internal solitary waves: The effect of background current[J]. Physics of fluids, 14(9): 2987-2999, 2002.

Stastna, M., &Peltier, W. R. On the resonant generation of large-amplitude internal solitary and solitary-like waves. J.Fluid Mech.,543(543), 267-292, 2005.

Stastna, M., Olsthoorn, J., Baglaenko, A., &Coutino, A. Strong mode-mode interactions in internal solitary-like waves. Phys.Fluids,27(4), 046604, 2015.

Talipova, T. G., Pelinovsky, E. N., &Kharif, C. Modulation instability of long internal waves with moderate amplitudes in a stratified horizontally inhomogeneous ocean. JETP Lett.,94(3), 182-186, 2011.

Terletska, K., Jung, K. T., Talipova, T., Maderich, V., Brovchenko, I., &Grimshaw, R. Internal breather-like wave generation by the second mode solitary wave interaction with a step. Phys.Fluids, 28(11), L03601-276, 2016.

Van der Boon C M. Numerical modelling of internal waves in the Browse Basin[D]. MSc Thesis, TU Delft, Delft, The Netherlands, 2011.

Venayagamoorthy, S. K., & Fringer, O. B. On the formation and propagation of nonlinear internal boluses across a shelf break. J. Fluid Mech., 577, 137-159, 2007.

Vlasenko, V., & Stashchuk, N.. Internal tides near the Celtic Sea shelf break: A new look at a well known problem. Deep Sea Research Part I: Oceanographic Research Papers, 103, 24-36, 2015.

Vlasenko, V., Stashchuk, N., Guo, C, & Chen, X. Multimodal structure of baroclinic tides in the South

China Sea. Nonlin. Processes in Geophys., 17(5), 529, 2010.

Wang, J., R. G. Ingram, and L. A. Mysak, Variability of internal tides in the Laurentian Channel. J. Geophys. Res., 96(C9), 16859–16875, doi:10.1029/91JC01580, 1991

Xu Z. H., B Yin, Y Hou, and Y Xu. Variability of internal tides and near-inertial waves on the continental slope of the northwestern South China Sea. J. Geophys. Res. Oceans, 118(1), 197–211, doi:10.1029/2012JC008212, 2013

Xu Z. H., K Liu, B Yin, Z Zhao, Y Wang, and Q Li. Long-range propagation and associated variability of internal tides in the South China Sea. J. Geophys. Res. Oceans, 121(11), 8268–8286, doi:10.1002/2016JC012105, 2016

Yang, Y. J., Fang, Y. C., Chang, M. H., Ramp, S. R., Kao, C. C., & Tang, T. Y. Observations of second baroclinic mode internal solitary waves on the continental slope of the northern south china sea. J.Geophys.Res.,114(C10), 637-644, 2009.

Yang, Y. J., Fang, Y. C., Tang, T. Y., & Ramp, S. R. Convex and concave types of second baroclinic mode internal solitary waves. Nonlinear Processes in Geophys.,*17*(6), 605-614, 2010.

Yuan, C., Grimshaw, R., & Johnson, E. The evolution of second mode internal solitary waves over variable topography. J.Fluid Mech., 836, 238-259, 2018.

Zhao, Z., Klemas, V., Zheng, Q., & Yan, X. Remote sensing evidence for baroclinic tide origin of internal solitary waves in the northeastern south china sea. Geophys.Res.Lett., 31(6), L06302, 2004.

Zhao, Z., & Alford, M. H. Source and propagation of internal solitary waves in the northeastern south china sea. J.Geophys.Res., 111(C11), 63-79, 2006.